# OPTIMUM DESIGN VIA PANDA2 OF COMPOSITE SANDWICH PANELS WITH HONEYCOMB OR FOAM CORES

David Bushnell
Senior Consulting Scientist (Retired)
Department H1-31, Building 255
Lockheed-Martin Palo Alto Research Laboratory
3251 Hanover St., Palo Alto, California 94304

## ABSTRACT

PANDA2 has been extended to handle panels with sandwich wall construction by inclusion of the following failure modes in addition to those previously accounted for: (1) face wrinkling, (2) face dimpling, (3) core shear crimping, (4) core transverse shear stress failure, (5) core crushing and tension failure, and (6) facesheet pull-off. Transverse shear deformation effects are included both for overall panel buckling and for local face sheet dimpling and face sheet wrinkling. The new PANDA2 code will optimize stiffened sandwich panels in which the stiffener segments as well as the panel skin may have sandwich wall constructions. The effects of panel buckling modal initial imperfections as well as initial face sheet waviness are accounted for during optimization cycles. The updated PANDA2 code will also handle optimization of a panel supported by an elastic Winkler foundation. Examples are presented for a uniformly axially compressed perfect and imperfect unstiffened panel without and with a uniform temperature gradient through the panel wall thickness. Initial face sheet waviness and initial overall buckling modal imperfections both have major influence on optimum designs of sandwich panels with honeycomb cores.

## INTRODUCTION

### Brief Review Of The Literature

Noor, Burton, and Bert [1] provide a recent survey of the state-of-the-art with regard to sandwich panels. Stein and his colleagues [2-4] have contributed several papers. The work reported here is based on earlier work by Vinson [5-7], Hoff and Mautner [8], Plantema [9], Hetenyi [10], and Bitzer and his colleagues at Hexcell Corporation [11-13]. The PANDA2 computer program for minimum weight design of unstiffened and stiffened flat and cylindrical panels and shells [14-20] is modified as described here. PANDA2 supercedes an earlier code PANDA [21] and contains algorithms adapted from BOSOR4 [22] in which the equations valid for branched shells of revolution are transformed to those valid for prismatic structures. PANDA2 will handle optimum designs of panels for which the panel skin stiffener module (module = one stiffener plus stiffener base plus panel skin on either side of the stiffener of total width equal to the stiffener spacing, as shown in Fig. 1) is in its locally postbuckled state (local buckling of the panel between adjacent stiffeners and of the stiffeners). The postbuckling theory in PANDA2 represents an extension of a theory first set forth by Koiter in 1946 [23]. Optimization is performed with use of the ADS software developed several years ago by Vanderplaats and his colleagues [24-25]. Although the examples presented here are for "classical" (non-composite) materials, PANDA2 will handle both regular and sandwich panels composed of laminated segments of advanced composite material [18,19]. PANDA2 consists of a "bundle" of executable processors, the most significant of which are:

| | |
|---|---|
| BEGIN | (user supplies starting design, material properties, boundary conditions) |
| DECIDE | (user chooses decision variables and lower and upper bounds for optimization) |
| MAINSETUP | (user supplies loads, strategy parameters, type of analysis to be performed, etc.) |
| PANDAOPT | (mainprocessor execution is launched) |

---

CHOOSEPLOT  (user chooses what to plot.)

DIPLOT  (plots are generated)

CHANGE  (user changes selected quantities)

SUPEROPT  (like PANDAOPT, except it attempts to find a global minimum-weight design [20])

STAGSMODEL  (a finite element model to be used in an execution of STAGS [17,26,27] is generated from an optimum design by PANDA2)

The purpose of the work on which this paper is based was to enhance PANDA2's capability to generate practical optimum designs of sandwich panels by inclusion of several new "sandwich-related" constraint conditions: face wrinkling, face dimpling, core shear crimping, core crushing, core normal tensile failure, face sheet pull-off, and core transverse shear stress failure. The very significant effects of initial face sheet wrinkling and initial buckling modal imperfections are included. This paper represents an abridged version of ITEM 271 in the file .../panda2/doc/panda2.news [29].

Meaning Of The Phrase, "Panel Module", And Other Panda2 Jargon

In the following discussion, the terms "module segment" and "nodal point" are used. Also the terminology, "Iseg" and "Dseg", occurs. "Iseg" and "Dseg" represent two panel module segment numbering schemes: "Iseg" used primarily with input (Fig. 1a) and "Dseg" referring to segment numbering in a discretized single skin-stringer panel module (Fig. 1b).

As described in previous papers, a stiffened panel is considered by PANDA2 to be built up of a series of identical modules, each of which is divided into segments, as depicted in Figs. 1(a) and (b) for a hat-stiffened panel. Any or all of the module segments can be of sandwich wall construction. Different materials can be used in different segments of the module.

In the PANDA2 literature "x" is the axial coordinate (normal to the plane of the paper), "y" is the coordinate normal to "x" and lying in the plane of the panel skin, and "s" is a coordinate similar to "y": normal to "x" and lying in the plane of each segment of the panel module cross section, as shown in Fig. 9 on p 492 of [14]. In

this paper "z" is the local through-thickness coordinate normal to the plane of each panel module segment.

## NEW SANDWICH-RELATED BEHAVIORAL CONSTRAINT CONDITIONS INTRODUCED INTO PANDA2

### Face Wrinkling

Face wrinkling is defined in the literature on sandwich shells as buckling of a face sheet supported on a continuous elastic foundation with a foundation modulus $K$ (e.g. lb/in$^3$). See Eqs.(2,3) for $K_{eff}$ which represents the effective stiffness of the sandwich core plus effective stiffness of the glue layer between the core and the face sheet. The elastic foundation modulus $K$ relates normal displacement $w$ of the face sheet to the pressure on that face sheet exerted by the core+glue material. The elastic foundation modulus depends on: 1. the thickness of the sandwich core, 2. the effective "normal-displacement" stiffness of the glue "layer" between a face sheet and the sandwich core, and, if the core is of honeycomb construction, on 3. the diameter of the honeycomb cell and 4. the thickness of the honeycomb cell wall. Three alternate formulas for face wrinkling are used in PANDA2:

(1) a formula based on Eq. (57) of [21] with the elastic foundation term added to $a_{33}$ (Eq.(55f) of [21]; see Eq.(37) below)

(2) a formula presented by Vinson [5], Eq.(4)

(3) a formula first derived by Hoff and Mautner [8] and presented by Plantema [9], Eqs.(5,6).

PANDA2 uses (1) and the minimum face wrinkling load factor computed from either (2) or (3). There is no post-face-wrinkling analysis included in PANDA2.

### Face Dimpling

Face dimpling is defined in the literature on sandwich shells as buckling of the face sheet over the diameter of a single cell of a honeycomb core. There is no post-face-dimpling analysis included in PANDA2.

### Core Shear Crimping

Core shear crimping is defined as overall buckling of the sandwich wall in a short-wavelength mode in which transverse shearing of the core predominates, as shown

in Fig. 3, p 1692 of Vinson's paper [5], Eqs.(9-11).

## Core Transverse Shear Stress Failure

Core transverse shear stress failure under transverse shear forces, $Q_x$ and $Q_y$ (e.g. lb/in) can occur when there is local bending of the panel, as is the case with axially compressed imperfect panels and panels subjected to normal pressure. This is not the same type of failure as "core shear crimping", a buckling phenomenon that can occur in a perfect, uniformly axially compressed flat panel for which the transverse shear forces $Q_x$ and $Q_y$ are zero. Rather, the new constraints for core failure under transverse shear forces $Q_x$ and $Q_y$ are analogous to stress constraints. New calculations for the transverse shear forces $Q_x$ and $Q_y$ are performed in PANDA2. It is assumed that the $Q_x$ and $Q_y$ are carried entirely by the sandwich core. The maximum values of $Q_x$ and $Q_y$ in each skin-stringer module segment, $Q_{x\,max}$ and $Q_{y\,max}$, are computed, and the corresponding maximum transverse shear stress components in the sandwich core, $\sigma_{13} = Q_{x\,max}/t_{core}$ and $\sigma_{23} = Q_{y\,max}/t_{core}$, in which $t_{core}$ is the thickness of the sandwich core, are compared to allowables that are now provided by the PANDA2 user as input data in "look-up" tables of experimentally determined core shear failure stress as a function of core density obtained from sandwich core manufacturers such as the Hexcel Corporation [13]. Initial facesheet waviness often has a dramatic influence on the sandwich core transverse shear stress margins.

## Core Crushing

Core crushing pressures are computed from the combined effects of axial and hoop curvature changes in each segment of the skin-stringer module which has a sandwich wall construction, applied normal pressure, amplification of initial facesheet waviness under load, and bending of initially imperfect stringer webs, especially stringer web bending along the lines of intersection of the stringer web with other parts of the skin-stringer panel module. The computed core crushing pressures are compared with allowables obtained, as in the case of sandwich core transverse shear stress allowables, from user-provided "look-up" tables. As is the case with core transverse shear stress, initial facesheet waviness has a dramatic influence on the sandwich core crushing margins.

## Face Sheet Pull-off And Core Normal Tension Failure

Face sheet pull-off and core tension failure (tension in the core normal to the plane of the sandwich panel module segment) are computed with use of formulas from Plantema [9] and from Hetenyi [10]. Initial facesheet waviness, stiffener web root bending, and hoop bending of initially imperfect cylindrical sandwich panels play major roles.

## Summary Of New Sandwich-related Design Margins

New design margins for a single segment of a panel module now appear in the PANDA2 output. These new "sandwich-related" margins are listed in Table.1. The margins with the string, "(VINSON)", are computed from Vinson's theory [5-7] The margins with the string "(HOFF)" are computed from a formula in Plantema's book [9]. PANDA2 uses only the minimum of the face wrinkling margins from "VINSON" and "HOFF". Therefore, both "VINSON" and "HOFF" face wrinkling margins never appear together for the same face sheet.

If more than one segment in a stiffened panel module consists of sandwich wall construction there can be many, many "sandwich-type" constraint conditions generated in a case. An example is presented in [29].

## THEORY

Some details on the theories on which the "sandwich-related" constraint conditions just listed are based follow.

## Overall Buckling Of The Sandwich Wall

The margin:

localbuck (VINSON) strng Iseg1 ....

is referred to by Vinson [5] as "Overall Instability" (of an unstiffened sandwich panel). Equations (2-6) in [5] govern. This mode of failure is called "localbuck" in PANDA2 because it represents buckling of a single segment of a skin-stringer module (panel skin or stringer web or under hat or hat crown) treated as a flat panel simply supported along all four edges. PANDA2 reserves the term "overall instability" or "general instability" to signify buckling in which the lines of intersection of stiffeners and panel skin displace normal to the panel skin in the buckling mode.

The "localbuck(VINSON)" margin provides a parallel prediction of what PANDA2 has always computed with analysis type IQUICK=1, that is, local buckling analysis of the panel module segments with use of Eq.(57) in [21] with subsequent "knockdown" as described in Section 8.2 of [14] to account for the effect of transverse shear deformation. For local buckling of the panel skin, the previously (and still) available PANDA2 margins that represent the same phenomenon as "localbuck(VINSON)" read:

buck.(DONL) simp-support local buck....

buck.(SAND) simp-support local buck....

in which the string "DONL" means "Donnell theory" and "SAND" means "Sanders theory".

For local buckling of various segments of the panel module other than the panel skin, the previously (and still) available PANDA2 margins that are analogous to the "localbuck(VINSON)" margin read:

buckling margin for stringer Iseg.3

in the case of the web of a T, J, or Hat stiffened panel, or

buckling margin for stringer Iseg.4

in the case of crown buckling in a Hat-stiffened panel. PANDA2's original local buckling constraints and Vinson's "localbuck(VINSON)" constraint are all still retained in the PANDA2 analysis because the effect of transverse shear deformation is handled differently in the two theories: in the original PANDA2 formulation the transverse shear deformation (t.s.d.) effect is applied as a "knockdown" factor as described in Section 8.2, pp495-496 in [14], whereas in Vinson's equations the effect of transverse shear deformation appears as quantities $V_x$ and $V_y$ in Eq.(3) of [5]. It is important that designs generated by PANDA2 survive the most conservative approximation of the buckling load factor obtained from various theories.

With use of analysis type IQUICK = 0 in PANDA2 (discretized single module model, see Figs. 3 - 5 on p.46 of [15]) the same local buckling phenomenon is identified by the phrase,

Local buckling from discrete model....

The "localbuck(VINSON)" margin is computed with the assumption that the module segment is flat and is simply supported along all four edges. Vinson uses certain coefficients in Eqs.(7) of [5] that depend on the number of axial halfwaves which he calls $n$. (In PANDA2 jargon this axial halfwavenumber is called $m$). If one assumes that there is only one-half wave across the width of the panel segment, then an explicit value for number of axial halfwaves $m$,

$$m = (a/b)(C_{55}/C_{44})^{1/4} \qquad (1)$$

results from minimization of the buckling load factor with respect to the number of axial halfwaves in the buckling mode. In Eq.(1) The quantity $a$ is the axial length of the panel module segment (length between adjacent rings if the module represents a stringer), $b$ is the "hoop" width of the panel module segment (for examples: stringer spacing, or width (height) of a stiffener web between the panel skin and outstanding flange, or width of the base or the crown of a hat), $C_{55}$ is the "hoop" (y or s) bending stiffness of the sandwich ($D_{22}$ in the usual laminated composite plate nomenclature), and $C_{44}$ is the axial (x) bending stiffness of the sandwich ($D_{11}$ in the usual nomenclature).

Strictly speaking the "localbuck(VINSON)" margin is valid only for uniaxial compression. However, in PANDA2 the application of Vinson's Eq.(2) in [5] is broadened to handle combined axial compression and in-plane shear in a panel skin because the "localbuck(VINSON)" buckling load factor (for the panel skin only) is "knocked down" by the same factor, FKNOCK(2), that accounts for in-plane shear and anisotropy in the computation of the local buckling margin obtained from the discretized single panel module model: "Local buckling from discrete model ".

Face Wrinkling

There are three margins for face wrinkling computed in PANDA2,

wrinkling; strng Iseg1....

wrinkling (VINSON);strng Iseg1....

wrinkling ( HOFF );strng Iseg1....

The first, "wrinkling strng", is computed from Eq.(57) of [21] (knocked down as described above to account for t.s.d.), with a term added to $a_{33}$ in Eq.(55f) of [21]

2166

to account for the effect of the elastic foundation represented by the sandwich core [see Eq.(37) in the "BUCPAN2" entry in the section, IMPLEMENTATION...] , which is treated as a Winkler elastic foundation with stiffness EFOUND (e.g. lb/in$^3$):

$$EFOUND = K_{eff} = \frac{1}{\left(1/K_{glue} + 1/K_{core}\right)} \quad (2)$$

in which the elastic foundation modulus of the sandwich core, Kcore, is assumed by PANDA2 to be

$$K_{core} = E_{core}^{eff} / \left(0.5 t_{core}\right) \quad (3)$$

where $E_{core}^{eff}$ is the effective elastic modulus of the sandwich core for displacements normal to the face sheets and $t_{core}$ is the thickness of the sandwich core. The "wrinkling strng" margin is valid for arbitrary combinations of in-plane face sheet loads: $N_x^{face}$, $N_y^{face}$, $N_{xy}^{face}$.

The second face wrinkling margin, "wrinkling (VINSON)", is computed from Eq.(15) in Vinson's paper [5] or Eq.(60) in Vinson's paper [6] (same right-hand-sides in both Vinson equations). In PANDA2 the equation is written in terms of face sheet resultants (e.g. $N_x^{face}$) and coefficients $C_{ij}$ of the 6 x 6 integrated constitutive law for each face sheet, which are available in SUBROUTINE BUCPAN, rather than in terms of stress and moduli, as is the case in Vinson's papers [5] and [6]. That is, in PANDA2 the critical face sheet resultants are given by:

$$N_x^{(face,crit)} = N_y^{(face,crit)} = N_{xy}^{(face,crit)} =$$

$$t_{face}\left[0.667\left(E_{core}/t_{core}\right)\left(C_{11}^{face}C_{22}^{face}\right)^{1/2}\right]^{1/2} \quad (4)$$

in which $C_{11}^{face}$ and $C_{22}^{face}$ are the axial and hoop integrated stiffness coefficients for a face sheet, $t_{core}$ is the thickness of the sandwich core, and $t_{face}$ is the thickness of a face sheet.

The third face wrinkling margin, "wrinkling ( HOFF )", is computed from a modified form of Eq.(10), p 43 of Plantema's book [9]:

$$N_x^{(face,crit)} = 0.5 t_{face}\left[\left(C_{11}^{face}/t_{face}\right)E_{core}G_{13}^{core}\right]^{1/3} \quad (5)$$

$$N_y^{(face,crit)} = 0.5 t_{face}\left[\left(C_{22}^{face}/t_{face}\right)E_{core}G_{23}^{core}\right]^{1/3} \quad (6)$$

$$N_{xy}^{(face,crit)} = N_y^{(face,crit)} \quad (7)$$

For combined in-plane loads, $N_x^{face}$, $N_y^{face}$, $N_{xy}^{face}$, the face wrinkling load factor (Eigenvalue) in PANDA2 corresponding to "wrinkling (VINSON)" is computed from

$$Eigenvalue = 1/[\left(N_x^{face}/N_x^{(face,crit)}\right)^2$$
$$+\left(N_y^{face}/N_y^{(face,crit)}\right)^2 + \left(N_{xy}^{face}/N_{xy}^{(face,crit)}\right)^2]^{1/2} \quad (8)$$

$N_x^{face}$ is the largest negative axial resultant in the face sheet of the current module segment, $N_y^{face}$ is the largest negative hoop resultant in the face sheet of the current module segment, and $N_{xy}^{face}$ is the largest absolute value of $N_{xy}^{face}$ in the segment. (See Table 14 for an example in which the face sheet resultants vary across the width of the panel module segment).

Face Sheet Dimpling

The face sheet dimpling load factor is governed by buckling of a simply-supported flat, square plate in which the hexagonal cell boundary is INSCRIBED. The length of one side of the square flat plate is 2*s, in which "s" is the width of one side of the regular hexagon of the honeycomb core. Equation [57] of [21], with subsequent "knockdown" to account for t.s.d., is used to compute the buckling load factor. Since the 2*s x 2*s simply supported square plate is larger than the actual hexagonal plate that dimples, This procedure should yield a conservative estimate for dimpling, provided that the local transverse shear deformation in the face sheet is properly accounted for. PANDA2's dimpling margins are valid for any combination, $N_x^{face}$, $N_y^{face}$, $N_{xy}^{face}$, of in-plane loading in composite, anisotropic face sheets.

Core Shear Crimping

Core shear crimping is computed from Vinson's Eq.(12) in [5] which, for axial compression, can be expressed in the form:

$$N_x^{(total,crit)} = G_{13}^{core} t_{core} \quad (9)$$

and for hoop compression or in-plane shear can be expressed in the analogous forms:

$$N_y^{(total,crit)} = G_{23}^{core} t_{core} \quad (10)$$

$$N_{xy}^{(total,crit)} = \left(G_{13}^{core} G_{23}^{core}\right)^{1/2} t_{core} \quad (11)$$

in which the subscript "total" denotes the sum of the corresponding resultants in the two facesheets. The other variables, $G_{13}^{core}$, $G_{23}^{core}$, and $t_{core}$, represent the x-z and y-z transverse shear moduli and the core thickness, respectively. For combined loads an equation analogous to Eq.(8) is used.

## New Configuration Constraints For Hexagonal Honeycomb Sandwich Core

For each panel module segment that is of hexagonal honeycomb core sandwich wall construction, two new constraint conditions of the following type have been added:

Face1 wavelength/celldiam;STR;Iseg=1...

Face2 wavelength/celldiam;STR;Iseg=1...

For each face sheet, the ratio

(face sheet wrinkling halfwavelength)/(1.732*s)

must be greater than or equal to 2.0 if the PANDA2 user indicates in "BEGIN" that he/she wants these constraints to be activated. In the expression above, the quantity "s" is the width of one side of the regular hexagonal honeycomb cell and 1.732*s is the flat-to-flat diameter of the hexagonal honeycomb cell. (1.732*s is called "cell size" in Hexcel Corporation's literature [11-13]). According to Plantema [9], the axial halfwavelength of the face wrinkles in an axially compressed sandwich plate is given by (face sheet wrinkling halfwavelength), $L$:

$$L = 1.26\pi\left[\left(C_{44}^{face}\right)^2 /\left(G_{xz}^{core} E_z^{core}\right)\right]^{1/6} \quad (12)$$

in which $C_{44}^{face}$ is the axial bending stiffness of the face sheet (D11 in the usual composite material nomenclature), $G_{xz}^{core}$ is the effective x-z transverse shear modulus of the sandwich core, and $E_z^{core}$ is the effective modulus of the sandwich core for stretching of the core normal to the facesheet (z-direction).

The configuration constraint,

$$L/(1.732s) \geq 2.0 \quad (13)$$

in which $L$ is the halfwavelength of the face sheet wrinkling mode of failure, was introduced into PANDA2 in order to force the honeycomb cell size to

be small enough so that Plantema's equations for the effect of initial face sheet waviness, to be discussed in the next subsection, become valid for honeycomb core sandwich panels. If constraints of the type (13) are imposed, then in the analysis of the effect of initial face sheet waviness (an effect that is significant if the characteristic wavelength of this initial waviness is the same as that of the face wrinkling mode of instability, which is the assumption used in PANDA2) the honeycomb core can be "smeared out", that is, treated as a homogeneous continuum in the computation of certain "sandwich-related" stress constraints to be discussed later in the subsection entitled "Additional New Sandwich-Related Stress Constraints".

Often imposition of the configuration constraint (13) does not significantly increase the optimum weight of a panel because the honeycomb cell wall thickness decreases in proportion to the honeycomb cell diameter. Also, small honeycomb cells are generally better than large cells because there are more surfaces for the facesheet-core adhesive to stick to, increasing the facesheet-core interface stress required to pull the facesheet from the core.

## Effect Of Initial Face Sheet Waviness

For normal (z-direction) stress and x-z and y-z transverse shear stress at the facesheet-core interface, Plantema (p 43, Eqs.(3) in [9]) gives the following equations as valid for a semi-infinite core:

$$\sigma_{z1} = \pi\left(w_0 / L\right)\left[1/(\lambda_1 - 1)\right]\left(G_{xz}^{core} E_z^{core}\right)^{1/2} \quad (14)$$

$$\tau_{xz1} = \pi\left(w_0 / L\right)\left[1/(\lambda_1 - 1)\right]G_{xz}^{core} \quad (15)$$

$$\tau_{yz1} = \pi\left(w_0 / L\right)\left[1/(\lambda_2 - 1)\right]G_{yz}^{core} \quad (16)$$

in which $w_0$ represents the amplitude of the initial face sheet waviness and $L$, the halfwavelength of the face wrinkling mode, is given above in Eq. (12). Plantema [9] writes that typical sandwich panels of good quality have $w_0 / L = 0.001$. In Eqs (14,15) $\lambda_1$ represents the load factor for face sheet wrinkling with all facesheet resultants, $N_x^{face}$, $N_y^{face}$, and $N_{xy}^{face}$, present. In Eq.(16) $\lambda_2$ represents the load factor for face sheet wrinkling with only the facesheet "hoop" resultant, $N_y^{face}$, present. The factors, $[1/(\lambda_i - 1)$, i=1,2], result from amplification of the initial face sheet waviness as the sandwich face sheets are subjected to destabilizing loads.

2168

The stresses, $\sigma_{z1}$, $\tau_{xz1}$, and $\tau_{yz1}$ play a significant role in the stress constraints to be discussed later in the subsection entitled "Additional New Sandwich-Related Stress Constraints".

### Effect Of Web Root And Tip Bending

If the IQUICK=0 model option (discretized single skin-stringer panel module model [14]) is used in the PANDA2 processors, MAINSETUP and PANDAOPT, and if a stringer-stiffened sandwich panel has an initial imperfection in the form of its local buckling mode, significant local face sheet pull-off stresses can develop in the top face sheet of the stringer base due to growth of the initial buckling modal imperfection as the panel is loaded. See, for example, the local buckling mode of the tee-stiffened panel shown in Fig. 4(b) on p. 46 of [15]. There can be significant bending in the imperfect web at its root where it intersects the top face sheet of the stringer base. (This web root bending is what gives rise to stringer popoff, as displayed in Figs. 5 and 6 on p 477 of [14]). A concentrated line moment,

$$M_0 = C_{55}^{web} w_{,ss}^{web} \tag{17}$$

is therefore applied to the top face sheet of the stringer base. In Eq.(17) $s$ is the width-wise coordinate in the web, identified in Fig. 9 on p 492 of [14].

If the stringer base is of sandwich construction, the line moment $M_o$ gives rise to a normal displacement distribution $w(y)$ in the face sheet of the stringer base adjacent to the stringer web. This $w(y)$ is antisymmetric with respect to the line of intersection of the stringer web and the stringer base. This face sheet is supported by an elastic foundation with stiffness $K$. Hetenyi in his article on beams on elastic foundations [10] gives for the normal stress at the beam facesheet-foundation interface:

$$\sigma_{z2} = Kw = M_0 \lambda^2 e^{-\lambda y} \sin(\lambda y) \tag{18}$$

in which

$$\lambda = \left[ K / \left( 4 C_{55}^{face} \right) \right]^{1/4} \tag{19}$$

Note that Hetenyi's formulas for a beam on an elastic foundation with a concentrated moment can be applied directly to the problem of a face sheet on an elastic foundation with a uniform applied line moment. Where Hetenyi uses $EI$ for the bending stiffness of the

facesheet of the beam, we can use $C_{55}^{face}$ for the "hoop" bending stiffness of the top face sheet of the stringer base.

The maximum normal stress, $\sigma_{z2}$, occurs at a distance $y = \pi / (4\lambda)$ from the line of intersection of the web root with with the top facesheet of the stringer base. The quantity $\sigma_{z2}$ in Eq.(18), with substitution of $y = \pi / (4\lambda)$, must be added to $\sigma_{z1}$ generated from amplification of the the initial face sheet waviness, Eq.(14). These normal stresses contribute to the total normal stress tending to crush the core or tending to cause normal tensile failure in the core or tending to pull the facesheet from the core.

An analogous line moment occurs at the tip of a stringer web where it intersects the outstanding flange of a TEE-shaped stringer.

The formulas above are valid for a semi-infinite elastic foundation. PANDA2 accounts for the finiteness of the depth of the elastic foundation in the case of a sandwich wall by "knocking down" the sum, $\sigma_{z1}$ plus $\sigma_{z2}$ by a factor that depends on the ratio $(\pi / \lambda) / t_{core}$, in which $t_{core}$ is the thickness of the sandwich core. If the ratio, $(\pi / \lambda) / t_{core}$, is less than unity the "knockdown" factor is unity; if the ratio, $(\pi / \lambda) / t_{core}$, is greater than 3.0 the "knockdown" factor is zero; and the "knockdown" factor is assumed to vary linearly between these two limits.

What if the stringer web is a rather thick sandwich wall? Then, rather than a single applied line moment $M_o$, PANDA2 assumes that there are equal and opposite line loads $P_1 = N_y^{webface1}$ and $P_2 = N_y^{webface2}$, applied to the top face sheet of the stringer base where the two local web face sheet resultants, $N_y^{webface1}$ and $N_y^{webface2}$, occur.

$P_1 = -P_2 = P = \pm N_y^{webface1}$ because there is zero net total hoop load $N_y^{totalweb}$ in the stringer web. Hetenyi [10] gives for the normal stress at the beam-foundation interface when the beam is subjected to a concentrated load:

$$\sigma_{z2} = Kw = 0.5 P \lambda e^{-\lambda y} \left[ \cos(\lambda y) + \sin(\lambda y) \right] \tag{20}$$

in which $\lambda$ is given above by Eq. (19). Rather than

compute the value of $y$ for which the maximum absolute value of $\sigma_{z2}$ occurs, in this case PANDA2 simply assumes the worst: that the two equal and opposite line loads, $P_1$ and $P_2$, applied by the two web face sheets to the top facesheet of the stringer base are far enough apart so that the maximum tensile or compressive normal stress, $\sigma_{z2}$, can with reasonable accuracy be given by

$$\sigma_{z2} = 0.5P\lambda \tag{21}$$

In order to generate conservative results, PANDA2 uses the following value for the line load $P$:

$$P = \pm\max\left[abs\left(N_y^{webface1}\right), abs\left(N_y^{webface2}\right)\right] \tag{22}$$

in which the superscripts "web face 1" and "web face 2" denote the maximum values anywhere in the stringer web face sheets rather than at the web face sheet roots only. This strategy also serves to smooth the optimization somewhat because very small changes in the dimensions of the stringer segments can sometimes lead to dramatic changes in the local buckling mode shape. An example of this behavior is displayed in Fig. 13 on p. 539 of [28]. The load factor for local buckling and the shape of the local buckling mode in the stringer web are the most significant determinants of $\sigma_{z2}$.

Additional New Sandwich-related Stress Constraints

Additional new sandwich-related stress constraints are also computed in SUBROUTINE BUCPAN of PANDA2. The new margins corresponding to these five additional "stress" constraints are identified in the PANDA2 output as listed in Table 2.

The "Iseg" number and the "Matl" number can be different from those listed in Table 2, of course, and "STR", which stands for "stringer", can just as well be "RNG", which stands for "ring"; and "MIDLENGTH", which corresponds to load Subcase 1, can just as well be "AT RINGS" or "PANEL END", which correspond to load Subcase 2 [17].

Sandwich core transverse shear stress constraints:

L-dir. sandwich core shear...

W-dir. sandwich core shear...

"L-dir" and "W-dir" are Hexcel Corporation jargon [11-13] denoting the major and minor sandwich core

transverse shear stiffnesses, denoted in PANDA2 Gcxz and Gcyz, respectively. In PANDA2 "L-dir" always coincides with the x-z transverse shearing plane and "W-dir" always coincides with the y-z or s-z transverse shearing planes of each module segment, in which the coordinate "y" or "s" is in the plane of the panel module segment and normal to the x (axial) direction, as displayed in Fig. 9 on p. 492 of [14].

In order to compute the new sandwich core transverse shear stress constraints, transverse shear resultants, $Q_x$ and $Q_y$ (e.g. lb/in), must first be obtained at every nodal point in the panel skin-stringer discretized single module. These transverse shear resultants, $Q_x$ and $Q_y$, are now computed in SUBROUTINE STRMID of the KOITER library in PANDA2 [15]. $Q_x$ and $Q_y$ are computed from the following equations for each discretized module segment:

$$Q_x = C_{44}w_{,xxx} + 3C_{46}w_{,xxy}$$
$$+\left(C_{45} + 2C_{66}\right)w_{,xyy} + C_{56}w_{,yyy} \tag{23}$$

$$Q_y = C_{46}w_{,xxx} + 3C_{56}w_{,xxy}$$
$$+\left(C_{45} + 2C_{66}\right)w_{,xyy} + C_{55}w_{,yyy} \tag{24}$$

in which $C_{44}, C_{45}, C_{46}, C_{55}, C_{56}, C_{66}$ are the integrated elastic constants for the module sandwich segment (elements of the 3x3 $D$ matrix in the usual nomenclature for laminated composite walls) and $w$ is the normal displacement field obtained from the KOITER branch of PANDA2 as described in [15]. The "triple derivatives", $w_{,xxx}$, $w_{,xxy}$, , etc., were not previously computed anywhere in PANDA2. Now the $W_{,xxx}$, $W_{,yyy}$, $W_{,xxy}$, $W_{,yyx}$ correponding to the local buckling mode $W$ (Note: uppercase $W$!) used in the KOITER branch are computed in SUBROUTINE MODE (MODE library) by backward differencing of $W_{,xx}$ and $W_{,yy}$. The quantity $W$ (cap $w$) denotes "normal local buckling modal displacement". The relation between $w$ (lower case) and $W$ (cap) is

$$w = fW \tag{25}$$

in which $f$ is the amplitude quantity obtained by solution of the nonlinear equations for the four unknowns, $f$, "a", M, N, in the KOITER branch of PANDA2 [15]. $f$ represents the amplitude of the postbuckling normal displacement field, "a" represents a postbuckling modal flattening parameter, "M" represents the slope of the postbuckling nodal lines, and

American Institute of Aeronautics and Astronautics

"N" is an axial wavelength parameter). Details about how the four unknowns, $f$, "a", M, and N, are determined in the KOITER branch are given in [15]. This postbuckling section in PANDA2 was very difficult to develop. It has been adjusted over a period of many years to increase its reliability.

PANDA2 computes (in SUBROUTINE STRMID) the maximum absolute values of the transverse shear stress components, $Q_x / t$ and $Q_y / t$, where $t$ is the total wall thickness of the module sandwich segment, for each skin-stringer module segment which has sandwich wall construction, then compares these two components of transverse shear stress with two user-provided allowable values for each sandwich core material used in the panel, as follows:

(sandwich core x-transverse shear stress constraint) =

$$\left[\tau_{xzcore}^{allowable} /\left(Q_x / t + \tau_{xz1}\right)\right] \quad (26)$$

(sandwich core y-transverse shear stress constraint) =

$$\left[\tau_{yzcore}^{allowable} /\left(Q_y / t + \tau_{yz1}\right)\right] \quad (27)$$

in which $\tau_{xz1}$ and $\tau_{yz1}$ are obtained from the analysis that accounts for initial face sheet waviness, Eqs. (15,16).

The $\tau_{xzcore}^{allowable}$ and $\tau_{yzcore}^{allowable}$ are obtained from user-provided "look-up" tables of values of core shear strength:

$$\tau_{xzcore}^{allowable} \text{ vs core density} \quad (28)$$

and

$$\tau_{yzcore}^{allowable} \text{ vs core density} \quad (29)$$

and

"knockdown factor for tau-allowable(core) vs core thickness" (30)

which originate in some published document such as Hexcel Corporation's [13]. An example of these user-provided "look-up" tables appears in Table 271.3 of ITEM 271 of [29].

Because the KOITER branch in PANDA2 does not handle transverse shear deformation effects in a

rigorous manner but via "knockdown" factors for effective bending stiffnesses of panel skin and stringer web(s) based on Timonshenko beam factors computed as described in Section 8.2 of [14] and via a "knockup" factor for the amplitude $f$ based on different values obtained for the local buckling load factor computed in the KOITER branch vs that computed from BOSOR4-type theory (See panda2.news ITEM 298 [29]), the values of the maximum transverse shear stresses, $Q_x / t$ and $Q_y / t$, obtained in the KOITER branch may be unconservative. Therefore, alternative values of $Q_x / t$ and $Q_y / t$ are computed in SUBROUTINE STRCON as described in panda2.news ITEM 294 [29]. PANDA2 uses the maxima of the values of $Q_x / t$ and $Q_y / t$ as computed in SUBROUTINE STRMID and as computed in SUBROUTINE STRCON.

Sandwich core crushing/tensile failure:

Core crushing margin....

sandwichcore tension margin....

Core crushing or tensile failure can occur from the combination of sandwich core normal stresses generated from the following phenomena:

1. Initial face sheet waviness: inward or outward initial face sheet waviness is amplified by the applied loading and tends to crush or pull apart the core locally [$\sigma_{z1}$ in Eq. (14)].

2. Bending at the root and tip of a stringer web in a panel with a finite local buckling modal initial imperfection: amplification of the initial local buckling modal imperfection may be associated with significant concentrated line loads where the stringer web intersects other parts of the structure that may have sandwich wall construction. These line loads give rise to local normal stresses at the facesheet core interface [$\sigma_{z2}$ in Eq.(18) or Eq.(21)].

3. Applied normal pressure to the panel skin: this pressure must be added to the other normal stress components tending to crush the core.

4. Deformation-induced core crushing or normal tension: Changes in curvature of initially flat panel segments always tend to crush the core. In the case of imperfect sandwich cylindrical panels and shells, curvature changes that increase the local hoop radius of

curvature give rise to tension in the core normal to the face sheets.

The contributions of Items 1 and 2 to core crushing/tensile failure have already been discussed. Item 3 requires no discussion. Next, we will address the question of deformation-induced core crushing/tensile failure.

Part of the core crushing/tensile pressure is induced by the development of changes in axial and hoop curvature as an imperfect, thermally and mechanically loaded panel deforms. The deformation-induced core crushing or tensile pressure is assumed in PANDA2 to be given by

$$P_{inducedcrush} = N_x^{face} / R_1 + N_y^{face} / R_2 \qquad (31)$$

in which $N_x^{face}$ is the axial resultant in the top face sheet caused by pure bending of the sandwich module segment about its neutral plane for axial bending; $R_1$ is the change in axial radius of curvature due to the pure bending (e.g. $w_{,xx} = 1/R_1$ in which w is the normal displacement resulting from pure bending)); $N_y^{face}$ is the hoop resultant in the top face sheet caused by pure bending of the sandwich module segment about its neutral plane for hoop bending; and $R_2$ is the change in hoop radius of curvature due to the pure bending (e.g. $w_{,yy} = 1/R_2$). For orthotropic face sheets with no "B" terms in the 6 x 6 integrated constitutive matrix, $N_x^{face}$ and $N_y^{face}$ can be expressed in terms of the two normal strain components, $\varepsilon_1^{face}$ and $\varepsilon_2^{face}$, at the top face sheet generated by pure axial and hoop bending, as:

$$N_x^{face} = C_{11}^{face}\varepsilon_1^{face} + C_{12}^{face}\varepsilon_2^{face} \qquad (32)$$

$$N_y^{face} = C_{12}^{face}\varepsilon_1^{face} + C_{22}^{face}\varepsilon_2^{face}$$

and the strain components, $\varepsilon_1^{face}$ and $\varepsilon_2^{face}$, for pure bending can be written in the form:

$$\varepsilon_1^{face} = \left[0.5\left(t - t_{face}\right) - C_{14}^{total} / C_{11}^{total}\right] / R_1 \qquad (33)$$

$$\varepsilon_2^{face} = \left[0.5\left(t - t_{face}\right) - C_{25}^{total} / C_{22}^{total}\right] / R_2$$

in which $t$ is the total thickness of the sandwich; $t_{face}$ is the thickness of the top face sheet; and $C_{ij}^{total}$ are elements of the integrated constitutive matrix for the entire sandwich wall. The ratio $-C_{14}^{total} / C_{11}^{total}$

represents the eccentricity of the neutral plane for axial (x) bending from the middle surface of the sandwich wall; $-C_{25}^{total} / C_{22}^{total}$ represents the same for "hoop" (y or "s") bending.

Equations (33) can be inserted into Eqs.(32), and the result can be inserted into Eq.(31) to yield the deformation-induced crushing pressure $p_{crush}$ in terms of the axial and hoop curvature changes, $1/R_1$ and $1/R_2$ (and $p_{tensile}$ in the case of initially curved sandwich panels with locally reduced curvature $1/R_2$).

In PANDA2 the maximum deformation-induced core crushing (tensile) pressure in each segment of the discretized skin-stringer single module is computed in SUBROUTINE GETEPS, which is called from SUBROUTINE STRTHK. In SUBROUTINE GETEPS the curvature changes, $1/R_1$ and $1/R_2$, are known. These curvature changes are associated with the local deformations normal to the module segment surface computed in the KOITER branch of PANDA2 [15] plus the local (prismatic) deformation that arises when a stringer-stiffened plate under normal pressure locally "wraps around" the line of intersection of the stringer web with the panel skin in the prebuckling phase (Figs. 56-58 in [14]).

As is true in the case of transverse shear stress components, $Q_x / t$ and $Q_y / t$, discussed above, the deformation-induced sandwich core crushing/ tensile pressure computed in SUBROUTINE GETEPS may be unconservative because this crushing/tensile pressure is derived from a displacement field determined from the KOITER branch in PANDA2, in which the effect of transverse shear deformation is accounted for in an approximate, possibly unconservative, manner. Therefore, an alternative value of the deformation-induced crushing/tensile pressure is also computed in SUBROUTINE STRCON as described in panda2.news ITEM 294 [29]. PANDA2 uses the maximum of the values of deformation induced crushing/tensile pressure calculated from the two alternative methods, as demonstrated in Parts 5a and 5b of Table 271.17 of ITEM 271 of [29].

Face Sheet Pull-Off

The constraints for face sheet pull-off are generated as described in the previous section. If PANDA2 perceives that the facesheet-core adhesive fails before the core, it identifies the corresponding normal tensile stress failure as "face sheet pull-off margin...." rather than as

"sandwichcore tension margin....".

## IMPLEMENTATION OF "SANDWICH" CAPABILITY IN PANDA2

PANDA2 permits analyses of sandwich walls with dissimilar face sheets and sandwich walls in which the in-plane loading in each face sheet may be different. Different loading in each of the two face sheets occurs in imperfect panels, thermally loaded panels with a temperature gradient through the sandwich wall, panels with applied external bending moments $M_x$ and $M_y$, panels with applied normal pressure, and panels that are in their locally postbuckled states.

In each module segment (see Figs. 1(a,b) for definition of a "module segment") there may be only one "core": the user cannot "stack" sandwich walls. If there is a "core" there cannot also be an "external" elastic foundation. By "external" is meant a core-like (relatively soft) material as the extreme layer of a segment. If there is an "external" elastic foundation there cannot also be a sandwich "core". There can only be a single "external" elastic foundation; the user may not embed a segment wall between two elastic foundations.

The user provides input data for each segment laminate as previously. The "external" elastic foundation or the sandwich "core" layer in each segment is provided by the user simply as a layer of the wall, just like any other layer in that wall. Then the user provides properties for the various materials in the structure just as previously. Up to this point the input data required for the BEGIN processor are the same as previously.

After the user has provided all the material properties, PANDA2 automatically searches through the layers of each module segment in order to identify possible candidates as sandwich cores or "external" elastic foundations. This search is performed in SUBROUTINE PANEL of the BEGIN library. The criterion for candidacy of a module segment layer to be treated as an elastic foundation or as a sandwich core material appears in the following code fragment in the "BEGIN" processor:

```
ENORM = SQRT(E1L(J)**2 + E2L(J)**2)

IF (ENORM/EMAX.LT.0.001

.AND.TL(J).GT.0.5*TWALL) THEN
```

```
        (ask user for elastic foundation
        modulus or core properties)

ENDIF
```

in which J is the Jth layer in a module segment; E1L and E2L are the lamina elastic moduli for deformation parallel and normal to the Jth lamina fibers, respectively; EMAX is the maximum value of ENORM for the segment laminate; TL is the thickness of an individual segment layer; and TWALL is the total segment laminate thickness. If the user wants a certain segment layer to be treated as an "external" elastic foundation or as a sandwich core, then he/she must:

1. supply a thickness for that layer which is at least half the thickness of the entire wall and

2. the square root of the sum of the squares of the moduli for axial and hoop stretching of the core must be smaller than 0.001 times EMAX, where EMAX is the square root of the sum of the squares of the moduli of the material of that layer which has the maximum value of ENORM for any of the layers in that segment laminate.

If the soft candidate material corresponds to an extreme layer of a module segment (that is, this layer actually represents an external elastic foundation), then the previously user-provided thickness of that layer is automatically reset to zero by PANDA2 so that in further PANDA2 processing that ("fake") layer does not contribute to the in-plane or bending stiffness of the segment laminate. NOTE: the weight of the elastic foundation is not included in PANDA2's computation of panel weight.

In order to implement the "sandwich/elastic foundation" capability into PANDA2, it was necessary to modify the PANDA2 prompt file, PROMPT.DAT, as listed in Table 271.1 of ITEM 271 of [29] and to modify the PANDA2 source code libraries, ARRAYS, BEGIN, BOSPAN, BUCKLE,... as described next.

### ARRAYS

Introduce a new subroutine FOUNDA (taken from BOSOR4) which computes the contribution of the elastic foundation to the local finite element stiffness matrix. SUBROUTINE STABIL was modified.

American Institute of Aeronautics and Astronautics

## BEGIN

Introduce new input data for sandwich core or external elastic foundation as called for in the modified PROMPT.DAT file (Table 271.1 of [29]). Reset previously user-supplied thickness for any layer representing an external elastic foundation to zero so that that "fake" layer will not affect in-plane or bending stiffness of the segment laminate. SUBROUTINE PANEL was modified.

## BOSPAN

Introduce the elastic foundation modulus K into the BOSOR4 model of the panel generated via the PANDA2 processor, PANEL. SUBROUTINE SEGMNT was modified.

## BUCKLE

Allow for a higher maximum allowable number of axial halfwaves in the local buckling model based on the discretized module. This is required because axially compressed plates on elastic foundations typically buckle into many, many axial halfwaves. SUBROUTINE LOCAL was modified. Also, include in SUBROUTINE CRIPPL (CRIPPL is called from SUBROUTINE STFEIG and performs local buckling of stiffener segments) the effect of an external elastic foundation, EFOUND=$K^i$. New quantities that govern the buckling load factors for stiffener segments are given for an "internal" stiffener segment by the following expressions. (An "internal" segment is a segment that is supported along both longitudinal edges by other stiffener segments or by the panel skin):

The new expression for the critical number of axial halfwaves $m_i$ in the $i$th locally buckled stiffener segment is given by:

$$m_i = \left[\left(K^i + C_{55}^i F^2\right)/C_{44}^i\right]^{1/4}(\ell/\pi) \qquad (34)$$

NOTE: $m_i$ in Eq.(34) (a wavenumber) is equal to the value of what is called "$m_i$" in Eq.(69) of [21] mu.ltiplied by $\ell/\pi$. The first term in the numerator on the right-hand side of Eq. (71) in [21] becomes

$$NUM_1 = 2\left[C_{44}^i\left(K^i + C_{55}^i F^2\right)\right]^{1/2} \\ +\left(C_{45}^i + 2C_{66}^i\right)F \qquad (35)$$

In Eqs.(34-35) the quantity $F$ is given by $(\pi/b_i)^2$, where $b_i$ is the width of the ith module segment. The quantity $\ell$ is the length between stiffeners. It was also necessary to modify SUBROUTINE WEBBUK (see panda2.news ITEM 121 [29]) to account for an elastic foundation. The simple modification is:

$$C44M4 = \left(C_{44}^i m_i^4 + K^i\right)/\left(C_{44}^i C_{55}^i\right)^{1/2} \qquad (36)$$

This simple modification holds because the elastic foundation modulus, $K_i$, called "EFOUND" in SUBROUTINE WEBBUK, contributes a "w-type" term to the strain energy analogous to the term $C_{44}^i m_i^4$ that represents the strain energy for axial bending. (See the similar kind of addition of EFOUND to the coefficient $a_{33}$ in SUBROUTINE EIGREG).

Also, in the case of hat stiffeners and truss-core sandwich panels, any elastic foundation that occurs as the first layer under the hat or as the first layer in the lower face sheet of a truss-core sandwich configuration is handled as if the elastic foundation material (called "FOAM" in the revised SUBROUTINE OBJECT) fills the hat or, in the case of a truss-core panel, fills the space between the lower and upper face sheets. The contribution of this "FOAM" is included in the computation of panel weight in SUBROUTINE OBJECT.

In addition, because of the extreme sensitivity of the sandwich core maximum transverse shear stress constraints to the local buckling mode shape predicted for the skin-stringer discretized module, it was necessary to introduce some iterative refinement in SUBROUTINE LOCAL, as described in panda2.news ITEM 301 [29].

## BUCPAN1

Compute buckling load factors corresponding to the new "sandwich-related" constraints listed above in the section entitled "SUMMARY OF NEW SANDWICH-RELATED MARGINS". A list of the new code is included in Table 271.2 of ITEM 271 of [29]. Most of the modifications in PANDA2 required for

implementation of the "sandwich" capability occur in SUBROUTINE BUCPAN.

---

## BUCPAN2

Introduce the elastic foundation modulus term, EFOUND=$K^i$, into the coefficient $a_{33}$ (see Eq. 55f, p. 553 of [21]). This term accounts for both the face wrinkling phenomenon in a sandwich wall as well as local buckling of the module segment with an "external" elastic foundation. SUBROUTINE EIGREG was modified as follows:

```
A33  =  C22*2.*FCUR/R**2  +
2.*C24*MSUM*FCUR/R
+2.*C25*NSUM*FCUR/R  +C44*(M14+M24)
+C55*(N14+N24)
+(2.*C45+4.*C66)*(N12*M12+M22*N22)  +
PREB  +  2.*EFOUND/C11SVE        (37)
```

in which the FORTRAN variables, FCUR, MSUM, NSUM, M14,...PREB, etc., are defined in SUBROUTINE EIGREG. NOTE: The elastic foundation modulus, EFOUND, is divided by C11SVE because the coefficients of the integrated constitutive law for the sandwich wall, [Cij, i,j=1,6], are normalized by C11SVE.

---

## GETCIJ

Compute integrated 6x6 constitutive matrices, $C_{ij}^{face1}$, $C_{ij}^{face2}$ corresponding to the local segment laminates that comprise face sheet 1 and face sheet 2 of each skin-stringer module segment judged by PANDA2 to be a sandwich wall. Compute face sheet laminate thicknesses, $t_{face1}$, $t_{face2}$ Compute effective transverse shear stiffnesses, $G_{13}^{face1}, G_{23}^{face1}, G_{13}^{face2}, G_{23}^{face2}$, of the two face sheets. Modifications were made to SUBROUTINES GETCIJ and OUTCIJ.

---

## KOITER

Introduce the elastic foundation contribution to the strain energy in a manner analogous to that done in ARRAYS and in BUCPAN2. The new terms associated with the elastic foundation contribution might well appear (for ease of implementation into PANDA2) in association with Eqs. (3) and (4), pp. 50 and 51, of [15], for the panel skin and the stringers, respectively. The strain energy of the elastic (Winkler) foundation is given by:

$$U_{foundation} = 0.5 \int Kw^2 dA \qquad (38)$$

which, for the panel skin, will cause to be added a term analogous to that in the first line of Eq.(45), p 62, [15], in which the coeffecient, $4N^2 D_{11}^{*i}$, is replaced by $0.25K.$. For the stringer the new contribution is analogous to the first term in Eq.(47), p. 62, [15], with the coefficient, $4N^2 C_{44}^i$, replaced by $0.25K$. SUBROUTINES EPSAVE, EIGKOI, GETBK, ENERGY were modified.

Also, SUBROUTINE KOIT2 was modified as described in panda2.news ITEM 298 [29] in order to compensate for the lack of a rigorous theory in the KOITER branch for the transverse shear deformation effect.

SUBROUTINE STRMID was modified to compute transverse shear forces, $Q_x$ and $Q_y$ (e.g. lb/in), at every nodal point in the discretized single panel skin-stringer module where the stresses are calculated. [See Eqs. (23-25)]. The maximum transverse shear stresses in each module segment, $Q_{x\,max}$ and $Q_{y\,max}$, are also computed. Later $Q_{x\,max}$ and $Q_{y\,max}$ are used, along with the user-provided "look-up" tables for allowable values, to generate constraint conditions for transverse shear stress failure of sandwich cores. [See Eqs.(26) - (30)].

---

## MODE

It was necessary to modify SUBROUTINE MODE to compute the "triple" derivatives of $W$ ( $W_{,xxx}$; $W_{,xxy}$; $W_{,yyx}$; $W_{,yyy}$) needed for computation of transverse shear forces, $Q_x$ and $Q_y$, and maximum transverse shear stresses, $Q_{x\,max}/t$ and $Q_{y\,max}/t$, corresponding to the growth of buckling modal initial imperfections. The $Q_{x\,max}/t$ and $Q_{y\,max}/t$ are required for building

American Institute of Aeronautics and Astronautics

the constraint conditions involving the maximum allowable x-z and y-z transverse shear stress components in the sandwich core in each panel module segment.

It was necessary to modify SUBROUTINE OUTPRS in order to compute the "triple" derivatives, WXXXGL and WYYYGL ("GL" for "global"), which are required for inclusion of the maximum x-z and y-z transverse shear stress components in the sandwich core of an unstiffened flat sandwich panel subjected to normal pressure.

The absolute values of the transverse shear stress components from growth of the buckling modal imperfections are added to those from normal pressure before the "L"-direction (x-z) and "W"-direction (y-z) sandwich core transverse shear stress constraints are calculated.

In addition, it was necessary to modify SUBROUTINE MODE to compute buckling modal derivatives for the "long-wavelength bending-torsion" mode, in order to compute the "triple" derivative ($W_{,yyy}$) required for computation of sandwich core transverse shear stress, in case the "long-wavelength bending-torsion" mode generates values of QXXMAX/t, QYYMAX/t that are greater in absolute value than the previously computed $Q_{x \, max} / t$ and $Q_{y \, max} / t$. (See panda2.news ITEM 302 [29] for more details).

PANCOM

Face wrinkling and dimpling mode shapes had to be initialized and new constraint phrases for "localbuck.", face wrinkling, face dimpling, and core shear crimping had to be introduced. SUBROUTINES PANCOM and RECORD were modified. New margins are recorded, as listed above in the section entitled "SUMMARY OF NEW SANDWICH-RELATED MARGINS" and in Part 3 of Table 6, for example.

SETUPC

Previously, the properties of materials used in the panel segment layers were assumed to be fixed. Because the

length "s" of one side of the hexagonal cell of the honeycomb core and the thickness "tc" of the honeycomb cell wall can now be decision variables, the properties, $G_{13}^{core}$, $G_{23}^{core}$, $\rho_{core}$, $E_{core}$ derived from these dimensions must now be recomputed every time the design is changed. Also, the effective elastic foundation modulus, EFOUND, of a sandwich core now depends upon the thickness of the core as well as on the dimensions "s" and "tc" of a honeycomb cell. For these reasons, SUBROUTINE SETUPC of the CONMAN library had to be extensively modified. (SUBROUTINE SETUPC takes the current values of the decision variables and design parameters and inserts them into their proper places in labelled common blocks).

STRAIN

The prebuckling in-plane resultants in the two face sheets of each module segment are computed from the already-computed stresses in the particular lamina of which the face sheets are composed. These face sheet resultants, $N_x^{face}$, $N_y^{face}$, $N_{xy}^{face}$, are called (FNXF1, FNXF2), (FNYF1, FNYF2), (FNXYF1, FNXYF2), respectively, in which "F1" and "F2" signify "face sheet 1" and "face sheet 2", respectively. A rather gross approximation is used in this part of PANDA2: Within any one face sheet of a given module segment, the minimum $N_x^{face}$ and minimum $N_y^{face}$ (maximum compressive values) for that face sheet and segment are combined with the maximum absolute value of $N_{xy}^{face}$ in that face sheet and segment. This extreme set $[N_x^{face}, N_y^{face}, N_{xy}^{face}]$ (from the point of view of stability) is assumed to be uniform over the entire segment. See Table 14 and associated discussion for an example. This "worst" approximation will always be conservative and may perhaps be too conservative in cases for which there is significant local bending caused by post-local buckling deformations or prebuckling bending in the neighborhoods of stiffeners, such as the "hungry horse" phenomenon described on p. 495 of [19]. PANDA2 will handle cases in which the $[N_x^{face}, N_y^{face}, N_{xy}^{face}]$ are different in each of the two face sheets of a segment.

SUBROUTINES STRTHK and GETEPS in the STRAIN library were also modified to compute the

deformation-induced sandwich core crushing pressure. (See discussion above associated with Eqs.(31) - (33)).

SUBROUTINE STRCON was modified to compute x-z and y-z transverse shear deformation stresses corresponding to deformations: $w_{,xxx}$, $w_{,xxy}$, $w_{,yyx}$, $w_{,yyy}$, which are now calculated for imperfect panels in SUBROUTINE CURIMP of the STRUCT library.

---

STOGET

Introduce new labelled common blocks as listed and defined in Table 271.2 of ITEM 271 of [29].

---

STRUCT

Certain quantities are initialized and new output is provided for the in-plane resultant set ($N_x, N_y, N_{xy}$) in each face sheet of each module segment judged by PANDA2 to be of sandwich wall construction. SUBROUTINE CURIMP, which predicts curvature changes and twist, $w_{,xx}, w_{,yy}, w_{,xy}$, in loaded imperfect panels, was modified to calculate also the deformations, $w_{,xxx}$, $w_{,xxy}$, $w_{,yyx}$, $w_{,yyx}$, required for later computation of transverse shear forces, $Q_{x2}$ and $Q_{y2}$, in SUBROUTINE STRCON of the STRAIN library. In SUBROUTINE SKIN the axisymmetric prebuckling transverse shear deformation, $w_{,xxx}$, is computed corresponding to the "hungry horse" [19] inter-ring deformations.

---

EXAMPLE: UNIFORMLY AXIALLY COMPRESSED, SIMPLY-SUPPORTED SANDWICH PLATE WITH TITANIUM FACESHEETS AND ALUMINUM HONEYCOMB CORE

Summary

Tables 3 - 18 and Figs. 2-12 pertain to this section. The case is named "vinson" in honor of Professor Jack Vinson of the Department of Mechanical and Aerospace Engineering at the University of Delaware.

The sandwich plate is unstiffened. The IQUICK = 0 (discretized) analysis [14,15] is used to obtain the results. In all of the examples the panel is subjected to uniform axial compression, $N_x$ = -5000 lb/in. First a perfect sandwich panel is optimized; then a sandwich panel with only initial face sheet waviness is optimized; then a sandwich panel with both initial face sheet waviness and a buckling modal initial imperfection is optimized; finally an imperfect (face sheet waviness plus initial buckling modal imperfection) sandwich panel with a uniform through-thickness temperature gradient in addition to the uniform axial compression is optimized.

Input Data

Table 271.3 of ITEM 271 in [29] lists the input data file, vinson.BEG, for the PANDA2 "BEGIN" processor. This input corresponds to an unstiffened, simply-supported, sandwich plate 100 inches long and 20 inches wide, with titanium face sheets and aluminum honeycomb core. The following material properties were used:

titanium face sheets:

$E$ =17.4*10$^6$ psi;  $v$ =0.3;  $\alpha$ =9.0*10$^{-6}$/deg.

$\rho$ = 0.16 lb/in$^3$,  $\sigma_{eff}^{allowable}$ = 120 ksi

aluminum honeycomb core material:

$E$ =10.0*10$^6$ psi;  $v$ =0.3;  $\alpha$ = 0;

$\rho$ = 0.10 lb/in$^3$ ,  $\sigma_{eff}^{allowable}$ = 40 ksi

Facesheet pull-off allowable= 40 lb/in.

The decision variables in the optimization are as follows:

T(1) = thickness of top face sheet

T(2) = thickness of honeycomb core

T(3) = thickness of bottom face sheet (Can be different from T(1)

s(2) = length of one side of regular hexagonal honeycomb core cell

tc(2)= thickness of wall of honeycomb cell wall

American Institute of Aeronautics and Astronautics

The decision variables "s" and "tc" have subscript "2" rather than "1" because these variables are associated with a material type and the the sandwich core is designated as "material type 2" in Table 271.3 of ITEM 271 of [29].

The lower bound of decision variable no. 4:

s(2): Length of one side of the hexagon

is set equal to 0.03608 in. because this corresponds to the smallest diameter honeycomb cell (1.732*s = 1/16th in.) fabricated in aluminum by the Hexcel Corporation, according to Table 13 in [13]. The lower bound of decision variable no. 5:

tc(2 ): Thickness of honeycomb cell wall

is likewise set equal to 0.0007 in.

In the starting design, the thickness of each face sheet is 0.03 inch and the thickness of the core is 0.5 inch. The initial values for the dimensions of a honeycomb cell are s = 0.5 inch and tc = 0.002 inch. Material No. 1 represents the material of the face sheets and Material No. 2 represents the material of the sandwich core. Table 271.3 of ITEM 271 of [29] contains a table of core crushing and L-direction and W-direction transverse shear stress allowables as functions of core density from [13], as well as other "look-up" tables for sandwich-related phenomena. These tables are not repeated here in order to save space.

The "INPUT DATA" section of ITEM 271 of [29] provides detail about how the PANDA2 user should provide initial values corresponding to the material type for the sandwich core, how PANDA2 uses these data to elicit further responses from the user concerning other properties of the sandwich core, and how PANDA2 converts the "sandwich-related" input data to data presented to the user in the output files. This information is deleted here to save space.

Results For Perfect Panel

Note that initially the honeycomb core configuration constraint, Eq.(13), is turned OFF and the initial face sheet waviness ratio $w_0 / L$ is set equal to zero. This is NOT recommended procedure for designing sandwich panels, but is done here for demonstration purposes. These factors have a major influence on the size of the cells of the optimized honeycomb core and therefore on the values of the "dimpling" and "wrinkling" margins.

In order to obtain an optimum design with PANDA2, the PANDA2 mainprocessor, invoked via the command "PANDAOPT", is first executed five times in succession in this particular case. This series of five executions generates a file called vinson.OPP, the end portion of which appears as Parts 1 and 2 of Table 3.

Part 3 of Table 3 lists the design margins that correspond to the optimum design listed in PART 2. Margins for buckling, wrinkling, dimpling, and core shear crimping are computed from equations of the type:

Buckling margin = (buckling load factor)/(f.s.) - 1.0
$$(39)$$

in which "f.s." denotes "factor of safety". Margins for stress are computed from equations of the type:

Stress margin = (allowablestress)/(stress*f.s.) - 1.0   (40)

Critical margins, that is, margins near zero, affect the evolution of the design in the neighborhood of the optimum. Note that at the optimum design the margin associated with sandwich core shear crimping (margin no. 9 in this case) is not critical.

Because the panel is perfect and there is no prebuckling bending, the top and bottom face sheets behave identically; therefore the wrinkling and dimpling margins for face sheet 1 are essentially the same as those for face sheet 2.

Margins 7 and 11 are obtained from the theory of [21] with the core represented as an elastic foundation as described in the discussion associated with Eq.(37), and with the effect of local transverse shear deformation in each facesheet included as described in Section 8.2 of [14]. Margins 8 and 12 are obtained from the Hoff-Mautner theory [8] as presented by Plantema [Eq.(5-7)]. No margins are listed in this case corresponding to the Vinson theory for face wrinkling because PANDA2 only chooses the most critical of the margins from EITHER the Hoff-Mautner [8] or the Vinson [5] theories.

Margins 10 and 13 are obtained from the theory of [21] for a simply supported square facesheet (no elastic foundation) with sides of length 2*s and with the local facesheet transverse shear deformation effect included as described in Section 8.2 of [14].

The design is deemed FEASIBLE even if there are

2178

some negative margins, provided that the absolute values of each negative margin is less than 0.01. If all negative margins are between -0.01 and -0.05, then the design is deemed ALMOST FEASIBLE. Designs with one or more negative margins less than -0.05 are deemed NOT FEASIBLE.

Note that margins 1, 2, 5, 6, and 14 in this case represent five predictions for the same phenomenon: overall buckling of the unstiffened panel. These margins are listed in Table 4. The three margins, 1, 2, and 6, are termed "local buckling" in PANDA2 because only the panel skin buckles. Phrases such as "overall buckling" or "general buckling" are reserved for buckling in which the lines of intersection of stiffener webs with the panel skin deflect in the buckling mode. Since there are no stiffeners in this example "local" buckling and "general" buckling point to the same phenomenon. The two margins, 1 and 2, are computed from the theories presented in [14] and [15]. The two margins, 5 and 14, are termed "general buckling" because the entire panel buckles. These two margins are computed with use of the theories presented in [21] and [20] (Donnell theory and Sanders theory, respectively), modified to account for transverse shear deformation as described in Section 8.2 of [14].

Ideally the five margins listed in Table 4 should all have the same value because they represent the same phenomenon. There is a significant discrepancy between the three margins, 1, 2, and 6, because the effect of transverse shear deformations (t.s.d.) is significant in this case and because the t.s.d. effect is handled differently in each of the three theories included in PANDA2 that lead to Margins 1, 2 and 6. Margin No. 1 is computed from a theory in which the transverse shear deformation effect is accounted for in the computation of the "Local buckling from discrete model" margin via a "knockdown" factor based on Timoshenko beam theory adjusted for a multiaxial stress field, as described in Sections 8.2 and 19.4 of [14], which most likely leads to conservative designs (see Fig. 25 in [14]). Margin No. 2 is computed from a theory implemented in the KOITER branch of PANDA2 in which the transverse shear deformation effect is accounted for by knocking down the bending stiffnesses by the Timoshenko factor. This is generally an unconservative method when the "knockdown" factor to compensate for transverse shear deformation effects is signficantly less than unity. However, note that the local deformations of imperfect panels with local buckling modal imperfections are computed including a strategy described in panda2.news ITEM

298 [29] which is intended to compensate for the lack of a rigorous transverse shear deformation theory in the KOITER branch of PANDA2. Margin No. 6 is computed from Vinson's theory as set forth in Eqs(2-6) of [5].

As will be seen from results to be presented later, the discrepancy between the buckling load factors from the various t.s.d. approximations diminishes for the more realistic cases in which the honeycomb core cell configuration constraint, Eq.(13), is active and there is initial face sheet waviness.

The two stress margins, Margin No. 3 and Margin No. 4, are calculated in two different subroutines of PANDA2, the first in SUBROUTINE STRTHK, which computes stresses corresponding to deformations obtained from the KOITER branch [15] of PANDA2, and the second in SUBROUTINE STRCON, which computes stresses from a much simplified theory in which it is assumed that initial buckling modal imperfections grow hyperbolically, as described in [19].

The results displayed in Figs. 2-12 for Design Iterations 0-20 show how the panel weight (the Objective) (Fig. 2), the Design Margins (Figs. 3-8), and the Design Parameters (Figs. 9-12) evolve during design iterations performed while the cell size constraint, Eq.(13), is turned OFF, there is no initial face sheet waviness ($w_0 / L = 0$), and there is no initial buckling modal imperfection ($w_{imp} = 0$). The results plotted at Iteration No. 20 correspond to those listed in Table 3.

The writer has found through exercise of PANDA2 for sandwich panels that very often the optimum design is not unique. Even in this very simple case of a perfect, unstiffened, uniformly axially compressed sandwich panel the optimum design is not unique. Different combinations of honeycomb cell size and cell wall thicknesses, "s" and "tc", affect the panel weight only slightly but have a major effect on the "dimpling" margins. Parts 4 - 7 in Table 3 demonstrate.

Following the initial optimization, the PANDA2 processor "CHANGE" was used to generate a new starting design with smaller values for hexagonal cell side width "s" and cell wall thickness "tc". The new starting values for "s" and "tc" are listed in Part 4 of Table 3. All other dimensions remain as listed in Part 2 of Table 3.

Part 5 of Table 271.9 in ITEM 271 of [29] lists the

optimization cycles resulting from four successive executions of PANDAOPT. Part 6 of Table 3 lists the new optimum design and panel weight. Note that although the panel weights from the two optimizations, 1.437E+01 in Part 2 and 1.440E+01 in Part 6, are the same to three significant figures, the two corresponding sets of "s" and "tc" are quite different:

After the first optimization (Part 2):

s(2)=2.361E-01, tc(2)=9.508E-04

After the second optimization (Part 6):

s(2)=1.757E-01, tc(2)=7.000E-04

All margins remain essentially the same after the second optimization (Parts 3 and 7) except the two face dimpling margins,

After the first optimization (Part 3):

10 -6.34E-04 dimpling of face 1

13 -6.34E-04 dimpling of face 2

After the second optimization (Part 7):

10 7.84E-01 dimpling of face 1

13 7.84E-01 dimpling of face 2

It is emphasized that for a design to be optimum all the margins need not be critical.

Vinson computes "optimum" design dimensions, "hc" (core thickness), "d" (inscribed diameter of hexagonal honeycomb cell), "tc" (thickness of cell wall), and "tf" (thickness of face sheet) from Eqs.(34 - 37) in [5]. For the panel with dimensions "a" x "b" = 100 x 20 in. and with titanium face sheets and aluminum core the "optimum" design from Vinson's Eqs.(34-37) is listed in Part 1 of Table 5. Corresponding to Vinson's "optimum" design PANDA2 obtains panel weight and design margins as listed in Parts 2 and 3 of Table 5. The word, optimum, is enclosed in quotation marks in this section because Vinson's "optimum" weight is considerably heavier than PANDA2's optimum: PANDA2 optimum = 14.37 lb; Vinson "optimum" = 20.75 lb. At the Vinson "optimum" the core crimping constraint is critical and the effective stress constraint is not (PART 3 of Table 5). In contrast, at the PANDA2

optimum the opposite holds (Part 3 of Table 3).

Note that the following three margins computed from from Vinson's theory (Vinson's "optimum" design):

6 -4.08E-02 localbuck (VINSON)....

8a-5.06E-04 wrinkling (VINSON)....

9 -2.94E-03 corecrimp (VINSON)....

are critical and that the margin

10 2.07E-01 dimpling of face 1

is somewhat higher than that computed by Vinson's Eq.(17). Vinson's Eq. (17) is not used in PANDA2 because it yields predictions for face sheet dimpling that are inconsistant with the classical Timoshenko equation for buckling of a square simply-supported plate of width and length b:

$$N_x^{crit} = 4\pi^2 Et^3 / \left[ 12(1 - v^2)b^2 \right] \quad \text{(Timoshenko) (41)}$$

For an isotropic material, Vinson's Eq.(17) is:

$$N_x^{dimpling} = 2Et^3 / \left[ (1 - v^2)d^2 \right] \quad \text{(Vinson) (42)}$$

For $b = d$, the Timoshenko formula predicts a dimpling load more than 50 per cent higher than that obtained from Vinson's formula. If we set $b$ in the Timoshenko formula equal to 2*s, where s is the length of one side of the regular hexagonal honeycomb cell, then we are assuming that the dimpling load factor is governed by buckling of a simply-supported flat, square plate in which the hexagonal cell boundary is INSCRIBED. Since this 2*s x 2*s simply supported square plate is larger than the actual hexagonal plate that dimples, it seems that such a procedure should yield a conservative estimate for dimpling, provided that transverse shear deformation effects are accounted for in a conservative manner.

Insertion of Vinson's "optimum" dimensions, 2*s = 2*0.40144 = $b$ and face sheet thickness $t = 0.031617$ (PART 1 of Table 5) and elastic modulus $E = 17.4$ x 10**6 psi and Poisson ratio $v = 0.3$ into the Timoshenko formula leads to $N_x^{crit} = 3084$ lb/in. Since the total applied axial compression, $N_x = 5000$ lb/in, is shared equally in this particular example by the two equal face sheets, a dimpling margin of 3084/2500 - 1 = 0.233 is indicated for each face sheet if the effect of

transverse shear deformation is neglected. Since the width/thickness ratio of the titanium face sheet over the dimple diameter in the Vinson "optimum" is about 25, transverse shear deformation effects are not significant for dimpling in this example.

The actual dimpling margin computed by PANDA2 is 0.207, as listed above and in Part 3 of Table 5. Therefore, PANDA2's dimpling computations are consistent with the Timoshenko formula for uniform axial compression, with a slightly lower margin than that just computed from the Timonshenko formula because there is a very small but finite effect of transverse shear deformation in the dimpling face sheet.

PANDA2's dimpling margins are valid for any combination, $N_x, N_y, N_{xy}$, of in-plane loading in composite, anisotropic face sheets because Eq.(57) on p. 553 of [21] is used for the computation.

If the same dimensions and properties are plugged into Vinson's Eq.(17), a dimpling margin very close to zero is obtained. This is to be expected, of course, because the "optimum" dimensions listed in PART 1 of Table 5 were derived from Vinson's equations, (34-37 of [5]), that require all four margins, localbuck (VINSON), wrinkling (VINSON), corecrimp (VINSON), and dimpling (VINSON), to be zero. Note that what Vinson calls "Overall Instability" on p. 1691 of [5] is called by PANDA2 "localbuck (VINSON)...".

Note that according to PANDA2, Vinson's "optimum" design is not feasible, since several margins are significantly negative, as follows:

5 -3.15E-01 buck.(DONL)....

8b-2.82E-01 wrinkling ( HOFF )....

12b-2.82E-01 wrinkling ( HOFF )....

18 -3.15E-01 buck.(SAND)....

Table 6 was generated after optimization with the "switch" for enforcement of the honeycomb core configuration constraint, Eq.(13), changed from "OFF" to "ON". As is to be expected, the effect of this constraint is to make the cell diameter, 1.732*s, and the depth of the sandwich core, T(2), significantly smaller. The optimum panel weight increases from 14.37 lbs to 15.33 lbs, about 6.7 per cent. In the case of a perfect panel without any initial face sheet waviness this

increase in weight is unnecessary. However, once we allow for initial face sheet waviness, then the "(facewrinkle halfwavelength)/celldiam > 2" constraint should always be turned on in order to ensure that the Plantema and Hetenyi theories described above are valid. That is, it is valid to represent the honeycomb core as an elastic continuum when computing the maximum facesheet-core interface normal and shear stresses generated by amplification of the initial face sheet waviness as load is applied to the panel.

Note that with the "(facewrinkle halfwavelength)/celldiam > 2" constraint turned on, the five margins that all represent overall buckling of this unstiffened panel are in reasonably close agreement, as demonstrated in Table 7. This is because the effect of transverse shear deformation is much smaller: the honeycomb core of the optimized panel is much stiffer under transverse shearing loads because the "(facewrinkle halfwavelength)/celldiam > 2" constraint was turned on before optimization, thereby forcing the cell size, 1.732*s, and the core depth, T(2), to become significantly smaller in this example.

The results displayed in Figs. 2-12 for Design Iterations 21-44 show the evolution of the design and margins of the perfect panel ( $w_0 / L = 0$, $w_{imp}$=0) with Eq.(13) turned ON. One can see from Fig. 3 that forcing the honeycomb cells to become smaller (see Fig. 11) results in a decrease in the discrepancy among the five models of overall panel buckling. The honeycomb core becomes thinner and has a higher transverse shear stiffness. Hence, transverse shear deformation effects are less dramatic than for the design at Iteration No. 20. Figures 7 and 8 show the large effect on wrinkling and dimpling margins: at the new optimum design at Iteration No. 44 the wrinkling, dimpling, and core shear crimping margins are not at all critical (Margins 7,9,10,11,12, 14, and 15 listed in Part 3 of Table 6).

Initial Face Sheet Waviness, $w_0 / L = 0.001$; Panel Otherwise Perfect

Table 8 presents a list of margins for the design at Interation No. 44 (Part 2 of Table 6):

T(1)=0.02087; T(2)=0.6137; T(3)=0.02087; s(2)=0.06766; $t_c(2)$=0.0007

but with the initial face sheet waviness, $w_0 / L$, increased from zero to 0.001, a value that Plantema [9] writes is typical for "smooth wings". Most of the

margins remain essentially the same. Those that are significantly affected by the introduction of finite initial face sheet waviness, $w_0 / L = 0.001$, are the core crushing margin, the x-z ("L-direction") core transverse shear stress margin, and the core tensile stress margin. (Compare Margins 16 and 17 in Table 6 with Margins 16 and 17 in Table 8 and note the new margin, Margin No. 19, in Table 8). With $w_0 / L = 0.0$ there are essentially zero core crushing and tensile stresses and x-z transverse shear stresses in the perfect panel. With $w_0 / L = 0.001$ there is significant core crushing stress and core tension stress as predicted from the Plantema equation, Eq.(14), and significant x-z ("L-direction") sandwich core transverse shear stress as predicted from the Plantema equation, Eq.(15).

With the print index, NPRINT = 2, in the vinson.OPT file (see Table 271.6 in ITEM 271 of [29]), PANDA2 lists the facesheet-core interface z-normal and x-z and y-z transverse shear stresses in the panel with initially wavy facesheets:

---

Action of web tending to crush the core or pull off the facesheet of Seg. 1: SIGWEB = $\sigma_{z2}$ = 0.0000E+00 (no stringer in this case)

Stress from web and initial waviness, matl= 2:
SIGTOT=SIGWEB+$\sigma_{z1}$=247.12 psi; $\tau_{xz1}$=108.53 psi;
$\tau_{yz1}$= 0.0294 psi

---

SIGWEB is generated from bending at the root of an initially imperfect stringer web (the imperfection has the shape of the local buckling mode, such as shown in Fig. 4b of [15]), as identified in the discussion associated with the Hetenyi equations, Eqs.(18 or 21). SIGWEB is zero in this case, of course, because there are no stringers. SIGTOT is equal to SIGWEB + $\sigma_{z1}$, in which $\sigma_{z1}$ is obtained from the Plantema equation, Eq.(14). $\tau_{xz1}$ and $\tau_{yz1}$ are obtained from the Plantema Eqs.(15,16). $\sigma_{z1}$, $\tau_{xz1}$, and $\tau_{yz1}$ arise from amplification of the initial facesheet waviness as the panel is compressed.

Table 9 lists the optimization cycles (Part 1), the

optimum design (Part 2), and the corresponding margins (Part 3) for the panel with initial face sheet waviness, $w_0 / L = 0.001$, and with the constraint, (face sheet wrinkling halfwavelength)/(1.732*s) > 2.0 turned ON. From Table 10 it is seen that with this more realistic case, at the optimum design the five margins, all of which represent the same phenomenon (overall buckling of this unstiffened sandwich panel), are now within a few per cent of eachother.

Also note that Margin No. 19 from Table 8,

19 1.71E+00 sandwichcore tension...

has been replaced by a differently worded margin in Table 9:

19 2.55E+00 face sheet pull-off...

This happened because PANDA2 tests for both tensile failure in the adhesive as well as tensile failure in the sandwich core material, using whichever yields the smaller margin. (In this case neither is critical).

Note that the face sheet wrinkling, face sheet dimpling, and core shear crimping margins are far from being critical at the optimum design.

The results displayed in Figs. 2-12 for Design Iterations 45-52 show the evolution of the design and margins of the panel with initial face sheet waviness, $w_0 / L = 0.001$, with Eq. (13) turned ON, and with no buckling modal initial imperfection ( $w_{imp}$=0). Inclusion of a finite (small) value for $w_0 / L$ results in a slight increase in panel weight (Fig. 2), a further decrease in the discrepancy among the five "overall panel buckling" margins (Fig. 3), a new critical margin: core crushing (Fig. 5), a somewhat thinner honeycomb core (Fig. 10), and a somewhat thicker honeycomb cell wall (Fig. 12).

In order to see what happens when initial face sheet waviness is present, but the constraint condition, (face sheet wrinkling halfwavelength)/(1.732*s) > 2.0 is turned OFF, the PANDA2 "CHANGE" processor was first used to set the sandwich hexagonal honeycomb core dimensions "s" and "$t_c$" to about four times their optimum values given in Part 2 of Table 9 and then the panel was re-optimized. The motivation behind this exploration was primarily to see how much influence on panel weight the presence of the "wrinkling/celldiameter" constraint has for a case in

which a reasonable level of initial facesheet waviness is present.

The results for the final optimum design are listed in Table 11. Note that the panel weight is essentially unaffected. The difference between 16.12 lbs (Part 2, Table 9) and 16.16 lbs (Part 1, Table 11) is in the optimization "noise" level. At the two optimum designs, the second with much bigger honeycomb cells, the ratio $s/t_c$ is about the same. Hence, margins governing overall stress and buckling of the unstiffened panel, core crushing, core shear crimping, face sheet wrinkling, and sandwich core transverse shear stress are essentially unaffected by the more than threefold increase in the size of the honeycomb cells. The margins for face sheet dimpling and face sheet pull-off are dramatically affected by the change, the face dimpling margin because of the much larger diameter of the honeycomb cells and the face sheet pull-off margin because there is much less core surface area for the facesheet-core interface adhesive to bond to. Table 12 highlights the quantities that are dramatically different at the two different optima listed in Tables 9 and 11.

Note from Part 2 of Table 11 that PANDA2 prints out a warning message in the *.OPM file if the half wavelength of the face wrinkling instability mode is smaller than the diameter of the hexagonal honeycomb cell.

### Imperfect Panel (Face Sheet Waviness + Initial Buckling Modal Imperfection)

In the simple example above, the sandwich panel is not loaded into its postbuckled state. Since the panel is "perfect" in the overall sense ("perfect" in quotes means there is initial face sheet waviness, $w_0 / L$, but that there is no initial overall buckling modal initial imperfection) and since the axial loading is uniform axial compression at the neutral plane, there is no overall bending of the panel under the axial compression and therefore the resultants in the two face sheets are equal to eachother and uniform. In a more elaborate case it may happen that, for one reason or another, a panel skin that is of sandwich construction will experience, in addition to initial face sheet waviness, considerable bending between stiffeners. In such a case the face sheet resultants, $N_x^{face}$, $N_y^{face}$,

$N_{xy}^{face}$ (called simply "Nx, Ny, Nxy" for lack of enough width in Table 14) may vary considerably over the width of the panel skin between stringers and may be

very different on the bottom face sheet ("facesheet 2") than they are on the top facesheet ("facesheet 1").

PART 2 of Table 9 lists thicknesses and honeycomb core dimensions "s" and "$t_c$" for the optimized panel with face sheet waviness, $w_0 / L = 0.001$, but otherwise perfect (zero overall buckling modal initial imperfection). Suppose the same optimized "perfect" panel with the same applied axial compression, Nx = -5000 lb/in, now has a buckling modal initial imperfection with amplitude $w_{imp} = 0.1$ in. Reference [19] describes how the effects of initial buckling modal imperfections are handled in PANDA2.

Table 13 lists the margins for the imperfect panel (initial face sheet waviness + overall initial buckling modal imperfection) with the same dimensions as the "perfect" panel (see Part 2 of Table 9, no further optimization yet). Several margins are now significantly negative because there is now considerable overall bending in the imperfect panel, with a result that the face sheets are no longer optimally loaded, each by a uniform axial compression, $N_x^{face} = -2500$ lb/in. Because of the overall bending of the panel as the initial buckling modal imperfection is amplified by the applied axial compression, the face sheets experience considerably more local axial compression than $N_x^{face} = -2500$ lb/in. Also present now in the face sheets are significant local hoop compression $N_y^{face}$ and in-plane shear $N_{xy}^{face}$. Hence, the face sheets now experience combined in-plane loads, $N_x^{face}$, $N_y^{face}$, $N_{xy}^{face}$, with the maximum local compressive $N_x^{face}$ now considerably exceeding -2500 lb/in. These "extra" local membrane loads in the face sheets of the imperfect sandwich panel cause several of the margins to become significantly negative. The design listed in Table 9 is no longer feasible because of the added overall initial buckling modal imperfection.

Table 14 shows a schematic of the unstiffened sandwich panel with segment and nodal point numbering (PART 1) and the actual distributions across the width of the panel and "worst" values of facesheet resultants, sandwich core transverse shear stress components, and deformation-induced core crushing pressures for the "PERFECT" (PARTs 2 and 3) and the IMPERFECT (PARTs 4 and 5) panel. The face sheet resultants, $N_x^{face}$, $N_y^{face}$, and $N_{xy}^{face}$ are called here "Nx, Ny, Nxy" for lack of sufficient width. In this

table,"x" is the axial coordinate and "y" is the "hoop" coordinate or (for stringer segments, if any) the "s" coordinate called out in Fig. 9 on p. 492 of [14].

In PANDA2 an unstiffened panel is modelled as shown in Fig. 6, p. 48 of [15]. The unstiffened panel is modelled in a manner analogous to that for a single discretized module of a blade-stiffened panel: symmetry conditions are imposed along the two longitudinal (unloaded) edges which are located midway between adjacent stringers, and constraint conditions are introduced to force the local buckling pattern to be approximately antisymmetric about the line of intersection of the stringer root with the panel skin. The buckling modal displacements of the unstiffened panel are artificially constrained to be antisymmetric at the midwidth (except for the axial displacement u), as shown in Fig. 6 of [15]. To repeat: the pattern of normal displacements w in an axially compressed panel with a buckling modal initial imperfection resembles that shown in Fig. 6 of [15]: symmetry conditions are applied along the two longitudinal (unloaded) edges of the panel and antisymmetry (classical simple support) conditions are applied at the panel midwidth. Admittedly, this is an unusual way to model a simply supported unstiffened flat plate. It is done this way in PANDA2 so that the same program code can be applied to both unstiffened and stringer-stiffened panels.

PART 2a of Table 14 lists face sheet resultants across the width of the "PERFECT" panel, and PART 2b lists the "worst" resultants from the point of view of stability. The "worst" resultants in a given panel module segment are assumed by PANDA2 to be uniform over that entire module segment for the purpose of calculation of face wrinkling, face dimpling, and core shear crimping load factors. In the case of the "PERFECT" panel the actual and assumed values are practically the same because the actual distributions are essentially uniform. (PANDA2 introduces a tiny imperfection amplitude when the user specifies no imperfection; that is why there is a small nonuniformity of $N_x^{face}$, $N_y^{face}$, and $N_{xy}^{face}$ across the width of the panel as listed in PART 2a).

Parts 3a and 3b give the width-wise distributions of x-z and y-z sandwich core transverse shear stresses and the "worst" values for the "PERFECT" panel. (The values are nonzero because of the tiny imperfection amplitude automatically supplied by PANDA2 in this case).

PART 4a of Table 14 lists face sheet resultants across

the width of the IMPERFECT panel, and PART 4b lists the "worst" resultants. Note that in this case the "worst" axial resultant Nx and hoop resultant Ny occur at the same points, but that the "worst" in-plane shear resultant Nxy occurs at different locations. Even so, PANDA2 assumes that all "worst" resultants in each module segment occur over that entire module segment. This is a conservative approximation. In this case the relatively small initial imperfection (amplitude = 0.1 in., which is about 16 per cent of the total panel thickness) has a huge effect because the panel dimensions correspond to the optimized "PERFECT" panel, for which buckling is almost critical as can be seen from the first margin listed in Part 3 of Table 9. Therefore, the initial buckling modal imperfection is greatly amplified by the applied load, with the result that very large additional face sheet resultants are generated in this particular case.

PARTs 5a and 5b of Table 14 list the actual distributions of sandwich core transverse shear stresses in the x-z and y-z planes for the imperfect panel. Again, the "worst" values are very large because of the extreme amplification of the buckling modal initial imperfection.

Because of the almost perfect antisymmetry of the buckling modal imperfection in this case, the top and bottom face sheets experience essentially the same "worst" face sheet resultants. That is why in the optimum design (Table 15) the top and bottom face sheets have the same thickness even though these two thicknesses are allowed to be independent decision variables.

Table 15 lists the final optimum design of the panel with initial face sheet waviness, $w_0 / L = 0.001$, and with initial buckling modal imperfection amplitude, $w_{imp} = 0.1$ in. Of course the re-optimized panel is somewhat heavier than that optimized without any initial buckling modal imperfection (Part 2 of Table 9). Note that the two face sheet thicknesses of the optimized imperfect panel are still equal. This is because both bottom and top face sheets "see" the same "worst" ("worst" = most destablizing) local membrane load combination, $N_x^{face}$, $N_y^{face}$, $N_{xy}^{face}$.

PANDA2 uses the "worst" face sheet prestress state in the computation of face wrinkling, face dimpling, and core crimping because these are all very local phenomena. It turns out that at the optimum design, face wrinkling, face dimpling, and core shear crimping

are no longer critical in this case, as can be seen from the margins listed in PART 4 of Table 15. The optimized imperfect panel is about 19 per cent heavier than the optimized "perfect" panel (panel with initial face sheet waviness, $w_0 / L = 0.001$, but with zero overall initial buckling modal initial imperfection.

The results displayed in Figs. 2-12 for Design Iterations 53-69 show the evolution of the design and margins of the panel with initial face sheet waviness, $w_0 / L = 0.001$, with Eq. (13) turned ON, and with a buckling modal initial imperfection, $w_{imp} = 0.1$ in. Inclusion of the buckling modal initial imperfection causes the panel to become significantly heavier (Fig. 2), the five "overall panel buckling" constraints to become non-critical (Fig. 3), both estimates of effective stress (Margins 3 and 4) to become critical (Fig. 4), the added presence of "L-direction" and "W-direction" sandwich core transverse shear stress margins that are not too far above critical values (Fig. 5), a significant increase in face sheet thickness (Fig. 9), a significant increase in honeycomb core thickness (Fig. 10), and an increase in thickness of the honeycomb cell wall (Fig. 12). Also, note that the evolution of several of the margins is much more "jumpy" than was the case for earlier design iterations performed with $w_{imp} = 0$ (Figs. 3, 5,10). This "jumpiness" is caused primarily by the high sensitivity of imperfect panel tangent stiffness components, $C_{11}^{tan}, C_{22}^{tan}, C_{33}^{tan}$, with a result that with each design iteration the buckling modal initial imperfection $w_{imp}$ is amplified by a different amount, giving rise to different stresses tending to crush the core or cause the core to fail in transverse shear.

Imperfect Panel With Through-thickness Temperature Gradient

Tables 16 - 18 list results for which there exist an initial face sheet waviness, $w_0 / L = 0/001$, an initial buckling modal imperfection with amplitude $w_{imp} = 0.1$ in., and a temperature gradient through the thickness of the sandwich that is uniform over the entire simply supported panel. The overall dimensions and properties of the panel are the same as listed in the previous tables.

These results represent a case in which the optimum design has different thicknesses in the top and bottom facesheets of the sandwich panel. This case is the same as that for the imperfect panel (the panel with both

initial face sheet waviness, $w_0 / L = 0.001$, and initial overall buckling modal imperfection, $w_{imp} = 0.1$ in.), except that now a uniform through-thickness thermal gradient has been added to the axial loading. The material properties are assumed to be independent of the temperature. The simply supported panel has nonzero thermal stresses in the facesheets because it is much longer than it is wide. If the bottom face sheet ("surface opposite stringer" in PANDA2 jargon even though there is no stringer in this case) is heated more than the top face sheet, which is the case corresponding to Tables 16 and 17, then before any axial load is applied to the sandwich plate, the bottom face sheet will be in axial compression and the top face sheet will be in axial tension due to the through-thickness thermal gradient. There are also smaller Poisson-ratio-induced hoop thermal stresses in the face sheets. This "thermal prestress" will cause the bottom face sheet to become thicker than the top face sheet during optimization cycles.

Note that in this example the thermal loading is considered to be part of "Load Set A", that is, the thermal loading is treated in the same way as the axial compression: thermal stresses, like the stresses from axial compression, are multiplied by the buckling eigenvalue (load factor) in the formulation of the bifurcation buckling problem.

Table 16 corresponds to the previously optimized imperfect panel, that is, the panel without any through-thickness thermal gradient (dimensions listed in the heading: the same panel as that identified in PART 4 of Table 15). Listed in Table 16 are the face sheet resultants of the imperfect panel with the applied axial load of -5000 lb/in and WITHOUT the thermal gradient (PART 1), the face sheet resultants of the imperfect panel with both the applied axial load of -5000 lb/in plus the thermal gradient (PART 2), and the margins when both the applied axial load and thru-thickness thermal gradient are present (PART 3). Note that the presence of the thru-thickness thermal gradient causes the effective stress margin of the bottom face sheet (layer 3) and the core crushing margin to become significantly negative: the optimum design obtained previously for the imperfect panel without the thru-thickness thermal gradient is no longer feasible if a through-thickness temperature gradient is present.

Table 17 lists results after optimization with the through-thickness thermal gradient present and with the bottom face sheet hotter than the top face sheet. As is to be expected from the results listed in Part 2 of Table 16

American Institute of Aeronautics and Astronautics

(bottom facesheet has higher destabilizing resultants than top facesheet), the bottom facesheet in the optimized design is much thicker than the top facesheet.

Global optima can be sought via the PANDA2 processor SUPEROPT [20]. This was done for this case with two thermal gradient options:

1. bottom face sheet hotter than top face sheet and

2. top face sheet hotter than bottom face sheet.

The results are listed in Table 18. It is seen that the optimum weights for the two cases are about the same as that listed in Table 17 and are practically the same for each of the two loading cases, as they should be. Presumably these are both very near the global optimum design.

Note that the optimum designs in PARTs 1 and 2 of Table 18 are not perfectly "symmetrical" with respect to which of the face sheets is the hotter. That is, all dimensions of the optimized designs should be the same except that the upper and lower face sheets should be exchanged. However, the lack of "symmetry" of the globally optimized designs with respect to which of the two face sheets is hotter is small, essentially in the "noise level" within which different designs display essentially the same weight and feasibility.

## CONCLUSIONS

Several new "sandwich-related" constraints have been added to the PANDA2 program. PANDA2 has been exercised for an axially compressed unstiffened sandwich panel which has initial face sheet waviness as well as a buckling modal initial imperfection. The face sheets of the sandwich panel need not be the same. A case involving optimization of an imperfect axially compressed panel with a uniform through-thickness temperature gradient, for which the optimum design has face sheets of unequal thickness, displays appropriate behavior.

If a buckling modal imperfection is present, overall buckling of the unstiffened panel is no longer critical (Fig. 3, Iterations 53-69). Rather, core crushing becomes critical and L-direction and W-direction core transverse shear stresses become nearly critical (Fig. 5, Iterations 53-69).

Face sheet dimpling and face sheet wrinkling become critical at optimized designs only if the honeycomb cell

size constraint, Eq. (13), is turned OFF (Figs. 6 and 7, Iterations 21-44).

If initial face sheet waviness, $w_0/L$, is nonzero, the weight of optimum designs is hardly affected by the presence or absence of the honeycomb cell size constraint, Eq. (13). Therefore, it is best always to obtain optimum designs with Eq. (13) turned ON and with a non-zero value for $w_0/L$ (Tables 9 and 11).

Optimization of sandwich panels with realistic assumptions, that is, with the honeycomb cell size constraint, Eq. (13) turned ON and with use of nonzero initial face sheet waviness, $w_0/L$, leads to minimum-weight designs for which the various approximations used in PANDA2 for including the effect of transverse shear deformations (t.s.d.) are in reasonably good agreement (Fig. 3, Iterations 40-50).

## ADDITIONAL WORK NEEDED

PANDA2 should be exercised for a wide variety of stiffened composite panels in which the various segments have sandwich wall construction.

Optimum designs obtained via PANDA2 should be checked by using STAGS to find collapse loads. The STAGS models should include, if possible, segments in which face sheet wrinkling, core crushing, core crimping, and core transverse stress failure as well as the effects of initial face sheet waviness, are predictable. As of this writing it is not possible to use STAGS to check "sandwich" designs generated via PANDA2.

More work needs to be done in PANDA2 on the effect of transverse shear deformation., especially in the routines that deal with the discretized panel module model and the routines that deal with stiffener rolling.

## ACKNOWLEDGMENTS

while the work was in progress. Dr. Frank Weiler helped the author produce the tables in two-column format.

## REFERENCES

[1] Noor, A. K., Burton, W. S., and Bert, C. W., "Computational models for sandwich panels and shells", Applied Mechanics Reviews, Vol. 49, No. 3, March 1996

[2] Stein, M. and Mayers, J., "A small deflection theory for curved sandwich plates", NACA Report 1008, 1951

[3] Stein, M. and Mayers, J., "Compressive buckling of simply supported curved plates and cylinders of sandwich construction, NACA TN-2601, 1952

[4] Stein, M. and Williams, J. G., "Buckling and structural efficiency of sandwich-blade stiffened composite compression panels," NASA Technical Paper 1269, September 1978

[5] Vinson, J. R., "Optimum design of composite honeycomb sandwich panels subjected to uniaxial compression", AIAA Journal, ol. 24, No. 10, October 1986

[6] Vinson, J. R., "Comparison of optimized sandwich panels of various constructions subjected to in-plane loads", Proceedings of First International Conference on Sandwich Constructions, Stockholm Sweden, pp 23-49, of SANDWICH CONSTRUCTIONS I, edited by K-A Olsson and R. P. Reichard, June 1989

[7] Vinson, J. R., "Analysis and optimization of composite and metallic sandwich cylindrical shells", Proceedings of Second International Conference on Sandwich Constructions, SANDWICH CONSTRUCTIONS II, Florida, March 1992

[8] Hoff, N. J. and Mautner, S. E., "The buckling of sandwich-type panels," Journal of Aerospace Sciences, Vol. 12, pp 285-297, July 1945

[9] Plantema, F. J., SANDWICH CONSTRUCTION, John Wiley, 1966

[10] Hetenyi, M., "Beams on Elastic Foundation", Chapter 3 of HANDBOOK OF ENGINEERING MECHANICS, edited by W. Flugge, McGraw-Hill, 1962

[11] Bitzer, T. N., "Aluminum honeycomb flatwise tensile strengths", Hexcel Corporation, Dublin, California, Report LSR 932480, January 1988

[12] Anon. "The basics of bonded sandwich construction", Hexcel Corporation, Dublin, California, Report TSB 124, January 1988

[13] Anon. "Mechanical properties of honeycomb material", Hexcel Corporation, Dublin, California, Report TSB 120, January 1988

[14] Bushnell, D., "PANDA2-Program for minimum weight design of stiffened, composite, locally buckled panels", Computers and Structures, Vol. 25 (1987) pp. 469-605.

[15] Bushnell, D., "Optimization of composite, stiffened, imperfect panels under combined loads for service in the postbuckling regime", Computer Methods in Applied Mechanics and Engineering, Vol. 103, pp 43-114 (1993)

[16] Bushnell, D., "Truss-core sandwich design via PANDA2", COMPUTERS AND STRUCTURES, Vol. 44, No. 5, pp 1091-1119 (1992)

[17] Bushnell, D. and Bushnell, W. D., "Minimum-weight design of a stiffened panel via PANDA2 and evaluation of the optimized panel via STAGS", Computers and Structures, Vol. 50, no. 4, p569-602 (1994)

[18] Bushnell, D. and Bushnell, W. D., "Optimum design of composite stiffened panels under combined loading", Computers and Structures, Vol. 55, No. 5, pp 819-856 (1995)

[19] Bushnell, D. and Bushnell, W. D.,"Approximate method for the optimum design of ring and stringer stiffened cylindrical panels and shells with local, inter-ring, and general buckling modal imperfections", Computers and Structures, Vol. 59, No. 3, pp. 489-527 (1996)

[20] Bushnell, D., "Recent enhancements to PANDA2" 37th AIAA Structures, Structural Dynamics and Materials Conference, April, 1996. Submitted to Finite Elements in Analysis and Design

[21] Bushnell, D., "Theoretical basis of the PANDA computer program for preliminary design of stiffened panels under combined in-plane loads," Computers and

Structures, Vol. 27, No. 4, pp 541-563 (1987)

[22] Bushnell, D., "BOSOR4: Program for stress, buckling, and vibration of complex shells of revolution," Structural Mechanics Software Series - Vol. 1, (N. Perrone and W. Pilkey, editors), University Press of Virginia, Charlottesville, 1977, pp. 11-131. See also Computers and Structures, Vol. 4, (1974) pp. 399-435; AIAA J, Vol. 9, No. 10, (1971) pp. 2004-2013; Structural Analysis Systems, Vol. 2, A. Niku-Lari, editor, Pergamon Press, Oxford, 1986, pp. 25-54, and Computers and Structures, 18, (3), (1984) pp. 471-536.

[23] Koiter, W. T., "Het Schuifplooiveld by Grote Overshrijdingen van de Knikspanning," Nationaal Luchtvaart Laboratorium, The Netherlands, Report X295, November 1946 (in Dutch)

[24] Vanderplaats, G. N., "ADS--a FORTRAN program for automated design synthesis, Version 2.01", Engineering Design Optimization, Inc, Santa Barbara, CA, January, 1987

[25] Vanderplaats, G. N. and Sugimoto, H., "A general-purpose optimization program for engineering design", Computers and Structures, Vol. 24, pp 13-21, 1986

[26] Almroth, B. O. and Brogan, F. A., The STAGS Computer Code, NASA CR-2950, NASA Langley Research Center, Hampton, VA (1978).

[27] Rankin, C. C., Stehlin, P.and Brogan, F. A.Koiter, W. T., Enhancements to the STAGS computer code. NASA CR 4000, NASA Langley Research Center, Hampton, VA (1986).

[28] Bushnell, D., "Nonlinear equilibrium of imperfect, locally deformed stringer-stiffened panels under combined in-plane loads", Computers and Structures, Vol. 27, No. 4, pp 519-539 (1987)

[29] Bushnell, D., ..../panda2/doc/panda2.news, a continually updated file distributed with PANDA2 that contains a log of all significant modifications to PANDA2 from 1987 through the present.

Table 1 New margins computed by PANDA2 especially for sandwich walls
============================================================

FOR FACE SHEET NO. 1 (top or leftmost face sheet):

wrinkling; strng Iseg1 ; MID;face 1; M=313;M=2;slope=0.;FS=1.
wrinkling (VINSON);strng Iseg1 ; MID;face 1; M=309;FS=1.
wrinkling ( HOFF );strng Iseg1 ; MID;face 1; M=309;FS=1.
dimpling; strng Iseg1 ; MID;face 1; M=1;M=1;slope=0.;FS=1.
Face1 wavelength/celldim;STR;Iseg=1 ;Mat1=2 ;MIDLENGTH;FS=1.

FOR FACE SHEET NO. 2 (bottom or rightmost face sheet):

wrinkling; strng Iseg1 ; MID;face 2; M=313;M=2;slope=0.,;FS=1.
wrinkling (VINSON);strng Iseg1 ; MID;face 2; M=309;FS=1.
wrinkling ( HOFF );strng Iseg1 ; MID;face 2; M=309;FS=1.
dimpling; strng Iseg1 ; MID;face 2; M=1;M=1;slope=0.,;FS=1.
Face2 wavelength/celldim;STR;Iseg=1 ;Mat1=2 ;MIDLENGTH;FS=1.

FOR ENTIRE SANDWICH WALL OR SANDWICH CORE OR BOTH FACESHEETS

localbuck (VINSON);strng Iseg1 ;MID; local buck.; M=5;FS=1.1
corecrimp (VINSON);strng Iseg1 ;MID; core crimping;FS=1.
core crushing margin;STR;Iseg=1 ;Mat1 2 ;MIDLENGTH;FS=1.
sandwichcore tension margin;STR;Iseg=1 ,Mat1 2 ,MIDLENGTH;FS=1.
L-dir. sandwich core shear;STR;Iseg=1 ,Mat1 2 ,MIDLENGTH;FS=1.
W-dir. sandwich core shear;STR;Iseg=1 ,Mat1 2 ,MIDLENGTH;FS=1.
face sheet pull-off margin;STR;Iseg=1 ,Mat1 2 ,MIDLENGTH;FS=1.
============================================================

Table 2 Additional new sandwich-related stress margins
============================================================

L-dir. sandwich core shear;STR;Iseg=1 ;Mat1 2 ;MIDLENGTH;FS=1.
W-dir. sandwich core shear;STR;Iseg=1 ;Mat1 2 ;MIDLENGTH;FS=1.
core crushing margin;STR;Iseg=1 ;Mat1 2 ;MIDLENGTH;FS=1.
sandwichcore tension margin;STR;Iseg=1 ,Mat1 2 ,MIDLENGTH;FS=1.
face sheet pull-off margin;STR;Iseg=1 ,Mat1 2 ,MIDLENGTH;FS=1.
============================================================

Table 3 INITIAL OPTIMIZATION OF PERFECT PANEL:
   1. No initial face sheet waviness;
   2. "(face sheet wrinkling halfwavelength)/(1.732*s) > 2.0"
      constraint condition turned OFF
   NOTE: 1. and 2. are NOT recommended practice but are done
         here for the purposes of demonstration.

PART 1: Original optimization

SUMMARY OF STATE OF THE DESIGN WITH EACH ITERATION
                          FOR EACH LOAD SET....
                                                     -----PANDAOPT-----
ITERA   WEIGHT                (IQUICK; NO. OF CRITICAL MARGINS)    5
TION    OF     LOAD SET NO.-> 1     2     3     4
NO.     PANEL  DESIGN IS...

| ITERATION NO. | WEIGHT OF PANEL | | | | | | | |
|---|---|---|---|---|---|---|---|---|
| 1 | 2.6001E+01 | FEASIBLE | (0; 0) | (0; 0) | (0; 0) | (0; 0) | (0; 0) | (0; 0) |
| 2 | 2.3366E+01 | FEASIBLE | (0; 2) | (0; 0) | (0; 0) | (0; 0) | (0; 0) | (0; 0) |
| 3 | 2.1934E+01 | FEASIBLE | (0; 4) | (0; 0) | (0; 0) | (0; 0) | (0; 0) | (0; 0) |
| 4 | 2.1003E+01 | FEASIBLE | (0; 4) | (0; 0) | (0; 0) | (0; 0) | (0; 0) | (0; 0) |
| 5 | 2.0314E+01 | FEASIBLE | (0; 5) | (0; 0) | (0; 0) | (0; 0) | (0; 0) | (0; 0) |
| 6 | 1.9788E+01 | FEASIBLE | (0; 4) | (0; 0) | (0; 0) | (0; 0) | (0; 0) | (0; 0) -----PANDAOPT |
| 7 | 1.9788E+01 | FEASIBLE | (0; 4) | (0; 0) | (0; 0) | (0; 0) | (0; 0) | (0; 0) |
| 8 | 1.8623E+01 | FEASIBLE | (0; 4) | (0; 0) | (0; 0) | (0; 0) | (0; 0) | (0; 0) |
| 9 | 1.7654E+01 | FEASIBLE | (0; 4) | (0; 0) | (0; 0) | (0; 0) | (0; 0) | (0; 0) |
| 10 | 1.6941E+01 | FEASIBLE | (0; 4) | (0; 0) | (0; 0) | (0; 0) | (0; 0) | (0; 0) |
| 11 | 1.6398E+01 | FEASIBLE | (0; 5) | (0; 0) | (0; 0) | (0; 0) | (0; 0) | (0; 0) |
| 12 | 1.5973E+01 | FEASIBLE | | | | | | -----PANDAOPT |

| | | | | | | | | |
|---|---|---|---|---|---|---|---|---|
| 13 | 1.5973E+01 | FEASIBLE | (0; 4) | (0; 0) | (0; 0) | (0; 0) | (0; 0) | (0; 0) |
| 14 | 1.5078E+01 | FEASIBLE | (0; 6) | (0; 0) | (0; 0) | (0; 0) | (0; 0) | (0; 0) |
| 15 | 1.4445E+01 | FEASIBLE | (0; 6) | (0; 0) | (0; 0) | (0; 0) | (0; 0) | (0; 0) |
| 16 | 1.4404E+01 | FEASIBLE | (0; 8) | (0; 0) | (0; 0) | (0; 0) | (0; 0) | (0; 0) |
| 17 | 1.4373E+01 | FEASIBLE | (0; 8) | (0; 0) | (0; 0) | (0; 0) | (0; 0) | (0; 0) <--optimum |
| 18 | 1.4395E+01 | FEASIBLE | (0; 9) | (0; 0) | (0; 0) | (0; 0) | (0; 0) | (0; 0) -----PANDAOPT |
| 19 | 1.4395E+01 | FEASIBLE | (0; 8) | (0; 0) | (0; 0) | (0; 0) | (0; 0) | (0; 0) |
| 20 | 1.4395E+01 | FEASIBLE | (0; 8) | (0; 0) | (0; 0) | (0; 0) | (0; 0) | (0; 0) -----PANDAOPT |

PART 2: Optimum design of perfect panel, no initial facesheet waviness;
        (face sheet wrinkling halfwavelength)/(1.732*s) > 2.0 constraint
        condition turned OFF; started from design with s(2)=0.5, tc(2)=0.002

VALUES OF DESIGN VARIABLES CORRESPONDING TO MINIMUM-WEIGHT DESIGN

| VAR. NO. | STR/ RNG NO. | SEG. NO. | LAYER NO. | CURRENT VALUE | DEFINITION |
|---|---|---|---|---|---|
| 1 | SKN | 1 | 1 | 2.087E-02 | T(5 )(SKN):thickness for layer index no.(1) |
| 2 | SKN | 1 | 2 | 8.218E-01 | T(2 )(SKN):thickness for layer index no.(2) |
| 3 | SKN | 1 | 3 | 2.087E-02 | T(3 )(SKN):thickness for layer index no.(3) |
| 4 | SKN | 1 | 0 | 2.361E-01 | s(2 )(SKN):Length of one side of the hexagon |
| 5 | SKN | 1 | 0 | 9.508E-04 | tc(2 )(SKN):thickness of honeycomb cell wall |

CORRESPONDING VALUE OF THE OBJECTIVE FUNCTION:

| VAR. NO. | STR./ RNG NO. | SEG. LAYER NO. | CURRENT VALUE | DEFINITION |
|---|---|---|---|---|
| 0 | 0 | 0 | 1.437E-01 | WEIGHT OF THE ENTIRE PANEL |

PART 3: Margins after original optimization; no initial facesheet waviness;
        (face sheet wrinkling halfwavelength)/(1.732*s) > 2.0 constraint
        condition turned OFF;

BUCKLING LOAD FACTORS FOR LOCAL BUCKLING FROM KOITER v. BOSOR4 THEORY:
Local buckling load factor from KOITER theory = 1.4376E+00
Local buckling load factor from BOSOR4 theory = 1.0598E+00

MARGINS FOR CURRENT DESIGN: LOAD CASE NO. 1, SUBCASE NO. 1

| MAR. NO. | MARGIN VALUE | DEFINITION |
|---|---|---|
| 1 | -1.76E-04 | Local buckling from discrete model-1.,M=5   axial halfwaves;FS=1.1 |
| 2 | 3.07E-01 | Local buckling from Koiter theory;M=6   axial halfwaves;FS=1.1 |
| 3 | 1.55E-03 | eff.stress:matl-1,SKN,Desg=2,node=11,layer=3,z=0.4345; MID.;FS=1. |
| 4 | 3.03E-03 | eff.stress:matl-1,SKN,Iseg=1,allnode,layer=3,z=0.4345;-MID.;FS=1. |
| 5 | 1.76E-03 | buck.(DONM)(VINSON);strng Iseg1 ;MID; local buck.; M=5;FS=1.1 |
| 6 | 1.75E-01 | localbuck (VINSON);strng Iseg1 ;MID; local buck.; M=5;FS=1.1 |
| 7 | 1.47E-01 | wrinkling ;strng Iseg1 ; MID;face 1; M=313;M=2;slope=0.;FS=1. |
| 8 | 2.08E-03 | wrinkling ( HOFF );strng Iseg1 ; MID;face 1; M=310;FS=1. |
| 9 | 9.57E-01 | corecrimp (VINSON);strng Iseg1 ;MID; core crimping;FS=1. |
| 10 | -6.34E-04 | dimpling ;strng Iseg1 ; MID;face 1; M=1;M=1;slope=0.;FS=1. |
| 11 | 1.47E-01 | wrinkling ;strng Iseg1 ; MID;face 2; M=313;M=2;slope=0.;FS=1. |
| 12 | 2.06E-03 | wrinkling ( HOFF );strng Iseg1 ; MID;face 2; M=310;FS=1. |
| 13 | -6.34E-04 | dimpling ;strng Iseg1 ; MID;face 2; M=1;M=1;slope=0.;FS=1. |
| 14 | 1.76E-03 | buck.(SAND);simp-support general buck;M=5;M=1;slope=0.;FS=1.1 |

PART 4: "CHANGE" processor used to restart from different values of
        hex cell side width "s" and hex cell thickness "tc"; vinson.CHG

| | | |
|---|---|---|
| n | | $ Do you want a tutorial session and tutorial output? |
| y | 4 | $ Do you want to change any values in Parameter Set No. 1? |
|   |   | $ Number of parameter to change (1, 2, 3, ...) |
| 0.800000E-01 |   | $ New value of the parameter(restart hex side width, s) |
| y | 5 | $ Want to change any other parameters in this set? |
|   |   | $ Number of parameter to change (1, 2, 3, ...) |
| 0.700000E-03 |   | $ New value of the parameter(restart hex cell thickness, tc) |
| n |   | $ Want to change any other parameters in this set? |
| n |   | $ Do you want to change values of "fixed" parameters? |
| n |   | $ Do you want to change values of allowables? |

Table 5  Results from PANDA2 for the optimum design obtained via Vinson's Eqs (34 - 37), pp1694-5, AIAA J. Vol. 24, 1986 [5]

PART 1:
VINSON'S OPTIMUM DESIGN DERIVED FROM EQS(34-37) in [5]

| LOWER BOUND | CURRENT VALUE | UPPER BOUND | DEFINITION |
|---|---|---|---|
| 1.00E-03 | 3.1617E-02 | 5.00E-01 | T(1 )(SKM):thickness for layer index no.(1) |
| 1.00E-01 | 1.2946E+00 | 4.00E+00 | T(2 )(SKM):thickness for layer index no.(2) |
| 1.00E-03 | 3.1617E-02 | 5.00E-01 | T(3 )(SKM):thickness for layer index no.(3) |
| 3.61E-02 | 4.0144E-01 | 3.00E+00 | s(2 )(SKM):Length of one side of the hexagon |
| 2.00E-04 | 5.2367E-04 | 1.00E-01 | tc(2 )(SKM):Thickness of honeycomb cell wall |

PART 2:
*************** DESIGN OBJECTIVE ***************
CORRESPONDING VALUE OF THE OBJECTIVE FUNCTION:

| VAR. NO. | STR/ RNG NO. | SEG. NO. | LAYER NO. | CURRENT VALUE | DEFINITION |
|---|---|---|---|---|---|
| | | 0 | 0 | 2.075E+01 | WEIGHT OF THE ENTIRE PANEL (Vinson's Optimum) |

PART 3:
MARGINS FOR CURRENT DESIGN: LOAD CASE NO. 1, SUBCASE NO. 1

| MAR. NO. | MARGIN VALUE | DEFINITION |
|---|---|---|
| 1 | 3.88E-01 | Local buckling from discrete model-1.,M-5  axial halfwaves;FS=1.1 |
| 2 | 1.70E+00 | Local buckling from Koiter theory,M=8  axial halfwaves,FS=1. |
| 3 | 5.14E-01 | eff.stress:matl-1,SKM,Dseg-2,node-11,layer-3,x=0.6789; MID.;FS=1. |
| 4 | 5.18E-01 | eff.stress:matl-1,SKM,Iseg-1,allnode,layer-3,x=0.6789;-MID.;FS=1. |
| 5 | -3.15E-01 | localbuck (VINSOM);strng general buck;M=5;M=1;slope=0.;FS=1. |
| 6 | -4.08E-02 | localbuck (VINSOM);strng Iseg1 ;MID; local buck.; M=5;FS=1.1 |
| 7 | -1.39E-02 | wrinkling ;strng Iseg1 ; MID;face 1; M-153;M=1;slope=0.;FS=1. |
| 8a | -5.06E-04 | wrinkling (VINSOM);strng Iseg1 ; MID;face 1; M-153;M=1;slope=0.;FS=1. |
| 8b | -2.82E-01 | wrinkling ( KOFF );strng Iseg1 ; MID;face 1; M-141;FS=1. |
| 9 | -2.94E-03 | corecrimp (VINSOM);strng Iseg1 ;MID; core crimping;FS=1. |
| 10 | -2.07E-01 | dimpling ;strng Iseg1 ; MID;face 1; M-1;M=1;slope=0.;FS=1. |
| 11 | -1.39E-02 | wrinkling ;strng Iseg1 ; MID;face 2; M-153;M=1;slope=0.;FS=1. |
| 12a | -5.08E-04 | wrinkling (VINSOM);strng Iseg1 ; MID;face 2; M-141;FS=1. |
| 12b | -2.82E-01 | wrinkling ( KOFF );strng Iseg1 ; MID;face 2; M-141;FS=1. |
| 13 | 2.07E-01 | dimpling ;strng Iseg1 ; MID;face 2; M-1;M=1;slope=0.;FS=1. |
| 14 | 5.90E+04 | Core crushing margin;STR,Iseg-1 ;Matl 1 ;MIDLENGTH;FS=1. |
| 15 | 4.12E+00 | L-dir. sandwich core shear;STR,Iseg-1 ;Matl 2 ;MIDLENGTH;FS=1. |
| 16 | 4.10E+00 | W-dir. sandwich core shear;STR,Iseg-1 ;Matl 2 ;MIDLENGTH;FS=1. |
| 17 | 2.19E+02 | (Max.allowable ave.axial strain)/(ave.axial strain) -1; FS=1. |
| 18 | -3.15E-01 | buck.(SAND);simp-support general buck;M=5;M=1;slope=0.;FS=1.1 |

Table 6  MORE OPTIMIZATION OF PERFECT PANEL: EQ.(13) CONSTRAINT TURNED ON
1. No initial face sheet waviness;
2. (face sheet wrinkling halfwavelength)/(1.732*s) > 2.0 constraint condition turned ON

PART 1: optimization (omitted here to save space. See Table 271.9 in ITEM 271 of [291]

PART 2: Optimum design of perfect panel, no initial facesheet waviness; (face sheet wrinkling halfwavelength)/(1.732*s) > 2.0 constraint condition turned ON.
VALUES OF DESIGN VARIABLES CORRESPONDING TO MINIMUM-WEIGHT DESIGN

| VAR. NO. | STR/ RNG NO. | SEG. NO. | LAYER NO. | CURRENT VALUE | DEFINITION |
|---|---|---|---|---|---|
| 1 | SKM | 1 | 1 | 2.087E-02 | T(1 )(SKM):thickness for layer index no.(1) |
| 2 | SKM | 1 | 2 | 6.137E-01 | T(2 )(SKM):thickness for layer index no.(2) |
| 3 | SKM | 1 | 3 | 2.087E-02 | T(3 )(SKM):thickness for layer index no.(3) |
| 4 | SKM | 1 | 0 | 6.766E-02 | s(2 )(SKM):Length of one side of the hexagon |
| 5 | SKM | 1 | 0 | 7.000E-04 | tc(2 )(SKM):thickness of honeycomb cell wall |

CORRESPONDING VALUE OF THE OBJECTIVE FUNCTION:

PART 5: Another optimization of perfect panel with "s" and "tc" reset via the PANDA2 processor called "CHANGE" to "s" = 0.08, "tc"=0.007 in.;
1. no initial face sheet waviness;
2. (face sheet wrinkling halfwavelength)/(1.732*s) > 2.0 constraint condition turned OFF;
(Results from optimization cycles are omitted here to save space. See Part 5 of Table 271.9 in ITEM 271 of [291])

PART 6: New optimum design; no initial face sheet waviness; (face sheet wrinkling halfwavelength)/(1.732*s) > 2.0 constraint condition turned OFF;
SUMMARY OF INFORMATION FROM OPTIMIZATION ANALYSIS

| VAR. NO. | DEC. VAR. | ESCAPE VAR. | LINK. VAR. | LINKED TO | LINKING CONSTANT | LOWER BOUND | CURRENT VALUE | UPPER BOUND | DEFINITION |
|---|---|---|---|---|---|---|---|---|---|
| 1 | Y | Y | Y | N | 0 | 0.00E+00 | 1.00E-03 | 2.0910E-02 | 5.00E-01 T(1) |
| 2 | Y | Y | Y | N | 0 | 0.00E+00 | 1.00E-01 | 8.2862E-01 | 4.00E+00 T(2) |
| 3 | Y | Y | Y | N | 0 | 0.00E+00 | 1.00E-03 | 2.0910E-02 | 5.00E-01 T(3) |
| 4 | Y | Y | | N | 0 | 0.00E+00 | 3.61E-02 | 1.7568E-01 | 3.00E+00 s(2) |
| 5 | Y | Y | | N | 0 | 0.00E+00 | 7.00E-04 | 7.0000E-04 | 1.00E-01 tc(2) |

CURRENT VALUE OF THE OBJECTIVE FUNCTION:

| VAR. NO. | STR/ RNG NO. | SEG. NO. | LAYER NO. | CURRENT VALUE | DEFINITION |
|---|---|---|---|---|---|
| | | 0 | 0 | 1.440E+01 | WEIGHT OF THE ENTIRE PANEL |

PART 7: Margins after second optimization; no initial face sheet waviness; (face sheet wrinkling halfwavelength)/(1.732*s) > 2.0 constraint condition turned OFF;

BUCKLING LOAD FACTORS FOR LOCAL BUCKLING FROM KOITER v. BOSOR4 THEORY:
Local buckling load factor from KOITER theory = 1.4389E+00
Local buckling load factor from BOSOR4 theory = 1.0991E+00

MARGINS FOR CURRENT DESIGN: LOAD CASE NO. 1, SUBCASE NO. 1

| MAR. NO. | MARGIN VALUE | DEFINITION |
|---|---|---|
| 1 | -8.10E-04 | Local buckling from discrete model-1.,M-5  axial halfwaves;FS=1.1 |
| 2 | 3.08E-01 | Local buckling from Koiter theory;M=6  axial halfwaves;FS=1.1 |
| 3 | 2.12E-03 | eff.stress:matl-1,SKM,Dseg-2,node-11,layer-3,x=0.4352;-MID.;FS=1. |
| 4 | 3.66E-03 | eff.stress:matl-1,SKM,Iseg-1,allnode,layer-3,x=0.4352;-MID.;FS=1. |
| 5 | 1.12E-03 | buck.(DOML);simp-support general buck;M=5;M=1;slope=0.;FS=1.1 |
| 6 | 1.75E-01 | localbuck (VINSOM);strng Iseg1 ;MID; local buck.; M=5;FS=1.1 |
| 7 | 1.44E-01 | wrinkling ;strng Iseg1 ; MID;face 1; M-313;M=2;slope=0.;FS=1. |
| 8 | -5.24E-04 | wrinkling (VINSOM);strng Iseg1 ; MID;face 1; M-309;FS=1. |
| 9 | 9.50E-01 | corecrimp (VINSOM);strng Iseg1 ;MID; core crimping;FS=1. |
| 10 | 7.84E-01 | dimpling ;strng Iseg1 ; MID;face 1; M-1;M=1;slope=0.;FS=1. |
| 11 | 1.44E-01 | wrinkling ;strng Iseg1 ; MID;face 2; M-313;M=2;slope=0.;FS=1. |
| 12 | -5.36E-04 | wrinkling ( KOFF );strng Iseg1 ; MID;face 2; M-309;FS=1. |
| 13 | 7.84E-01 | dimpling ;strng Iseg1 ; MID;face 2; M-1;M=1;slope=0.;FS=1. |
| 14 | 1.12E-03 | buck.(SAND);simp-support general buck;M=5;M=1;slope=0.;FS=1.1 |

Table 4  Five margins computed in PANDA2 which, for the special case of the unstiffened flat panel, denote the same phenomenon: Overall panel buckling. Perfect panel, no initial waviness, Eq. (13) constraint turned OFF.

| 1 | -1.76E-04 | Local buckling from discrete model-1.,M-5  axial halfwaves;FS=1.1 |
|---|---|---|
| 2 | 3.07E+01 | Local buckling from Koiter theory,M=6  axial halfwaves;FS=1.1 |
| 5 | 1.76E-03 | buck.(DOML);simp-support general buck;M=5;M=1;slope=0.;FS=1.1 |
| 6 | 1.75E-01 | localbuck (VINSOM);strng Iseg1 ;MID; local buck.; M=5;FS=1.1 |
| 14 | 1.76E-03 | buck.(SAND);simp-support general buck;M=5;M=1;slope=0.;FS=1.1 |

**VAR. STR/ SEG. LAYER  CURRENT**
**NO.  RNG  NO.  NO.  VALUE      DEFINITION**
0  0  0  1.531E+01  WEIGHT OF THE ENTIRE PANEL

**PART 3:** Margins after optimization; no initial facesheet waviness;
(face sheet wrinkling halfwavelength)/(1.732*s) > 2.0 constraint
condition turned ON;
vinson.OPM (abridged)

**BUCKLING LOAD FACTORS FOR LOCAL BUCKLING FROM KOITER v. BOSOR4 THEORY:**
Local buckling load factor from KOITER theory = 1.2219E+00
Local buckling load factor from BOSOR4 theory = 1.1000E+00

**MARGINS FOR CURRENT DESIGN: LOAD CASE NO. 1, SUBCASE NO. 1**

| MAR. MARGIN | | |
|---|---|---|
| NO. | VALUE | DEFINITION |
| 1 | -4.65E-06 | Local buckling from discrete model-1.,M=5  axial halfwaves;FS=1.1 |
| 2 | 1.11E-01 | Local buckling from Koiter theory,M=5  axial halfwaves;FS=1. |
| 3 | 2.26E-03 | eff.stress:matl=1,SKN,Dseg=2,node=11,layer=3,x=0.3283; MID.;FS=1. |
| 4 | 2.81E-03 | eff.stress:matl=1,SKN,Iseg-1,allnode,x=0.3283;-MID.,FS=1. |
| 5 | 2.97E-03 | buck.(DONL);simp-support general buck;M=5;M=1;slope=0.;FS=1.1 |
| 6 | 6.39E-02 | localbuck (VINSON);strng Iseg1 ;MID; local buck.; M=5;FS=1.1 |
| 7 | 1.09E+00 | wrinkling ;strng Iseg1 ; MID;face 1; M=445;M=1;slope=0.;FS=1. |
| 8 | 2.12E-03 | Face1 wavelength/celldiam;STR;Iseg=1 ;Matl=2 ;MIDLENGTH;FS=1. |
| 9 | 9.90E-01 | wrinkling ( NOFF );strng Iseg1 ;MID; core crimping;FS=1. |
| 10 | 2.77E+00 | corecrimp (VINSON);strng Iseg1 ;MID; core crimping;FS=1. |
| 11 | 8.88E+00 | dimpling ;strng Iseg1 ; MID;face 1; M=1;M=1;slope=0.;FS=1. |
| 12 | 1.09E+00 | wrinkling ;strng Iseg1 ; MID;face 2 ; M=445;M=1;slope=0.;FS=1. |
| 13 | 2.12E-03 | Face2 wavelength/celldiam;STR;Iseg=1 ;Matl=2 ;MIDLENGTH;FS=1. |
| 14 | 8.90E-01 | wrinkling ( NOFF );strng Iseg1 ; MID;face 2; M=1;M=1;slope=0.;FS=1. |
| 15 | 8.88E+00 | dimpling ;strng Iseg1 ; MID;face 2; M=1;M=1;slope=0.;FS=1. |
| 16 | 1.21E+06 | Core crushing margin;STR;Iseg=1 ;Matl 2 ;MIDLENGTH;FS=1. |
| 17 | 2.35E+02 | L-dir. sandwich core shear;STR;Iseg-1 ;Matl 2 ;MIDLENGTH;FS=1. |
| 18 | 1.44E+02 | W-dir. sandwich core shear;STR;Iseg=1 ;Matl 2 ;MIDLENGTH;FS=1. |
| 19 | 1.44E+02 | (Max.allowable ave.axial strain)/(ave.axial strain) -1; FS=1. |
| 20 | 2.97E-03 | buck.(SAND);simp-support general buck;M=5;M=1;slope=0.;FS=1.1 |

**Table 7** Five margins computed in PANDA2 which, for the special case of the unstiffened flat panel, denote the same phenomenon: Overall panel buckling. This table is analogous to Table 4.

| | | |
|---|---|---|
| 1 | -4.65E-06 | Local buckling from discrete model-1.,M=5  axial halfwaves;FS=1.1 |
| 2 | 1.11E-01 | Local buckling from Koiter theory,M=5  axial halfwaves;FS=1. |
| 5 | 2.97E-03 | buck.(DONL);simp-support general buck;M=5;M=1;slope=0.;FS=1.1 |
| 6 | 6.39E-02 | localbuck (VINSON);strng Iseg1 ;MID; local buck.; M=5;FS=1.1 |
| 20 | 2.97E-03 | buck.(SAND);simp-support general buck;M=5;M=1;slope=0.;FS=1.1 |

**MARGINS FOR CURRENT DESIGN: LOAD CASE NO. 1, SUBCASE NO. 1**

| MAR. MARGIN | | |
|---|---|---|
| NO. | VALUE | DEFINITION |
| 1 | -4.27E-03 | Local buckling from discrete model-1.,M=5  axial halfwaves;FS=1.1 |
| 2 | 1.06E-01 | Local buckling from Koiter theory,M=5  axial halfwaves;FS=1.1 |
| 3 | 1.18E-03 | eff.stress:matl=1,SKN,Dseg=2,node=11,layer=3,x=0.3277; MID.;FS=1. |

**Table 8**

Margins before optimization; Initial facesheet waviness, w0/L = 0.001;
(face sheet wrinkling halfwavelength)/(1.732*s) > 2.0 constraint
condition turned ON;
vinson.OPM file (abridged) corresponding to the optimum design found
for no initial facesheet waviness:
T(1)=0.02087; T(2)=0.6137; T(3)=0.02087; s(2)=0.06766; tc(2)=0.0007

---

**PART 1:** Optimization, starting from optimized panel obtained with the
initial face sheet waviness, w0/L = 0.0 and with the constraint:
(face sheet wrinkling halfwavelength)/(1.732*s) > 2.0
turned ON. Starting design:
T(1)=0.02087; T(2)=0.6137; T(3)=0.02087; s(2)=0.06766; tc(2)=0.0007
In this case the initial face sheet waviness, w0/L = 0.001.

**SUMMARY OF STATE OF THE DESIGN WITH EACH ITERATION**
**FOR EACH LOAD SET....**

| ITERA-TION NO. | WEIGHT OF PANEL | LOAD SET NO.--> DESIGN IS... | (IQUICK; NO. OF CRITICAL MARGINS) | | | | |
|---|---|---|---|---|---|---|---|
| | | | 1 | 2 | 3 | 4 | 5 |
| | | | | | --PANDAOPT-- | | |
| 1 | 1.531E+01 | NOT FEASIBLE | (0; 7) | (0; 0) | (0; 0) | (0; 0) | (0; 0) |
| 2 | 1.732E+01 | NOT FEASIBLE | (0; 1) | (0; 0) | (0; 0) | (0; 0) | (0; 0) |
| 3 | 1.720E+01 | FEASIBLE | (0; 1) | (0; 0) | (0; 0) | (0; 0) | (0; 0) |
| 4 | 1.682E+01 | FEASIBLE | (0; 5) | (0; 0) | (0; 0) | (0; 0) | (0; 0) |
| 5 | 1.611E+01 | ALMOST FEASIBLE | (0; 8) | (0; 0) | (0; 0) | (0; 0) | (0; 0) |
| 6 | 1.613E+01 | ALMOST FEASIBLE | (0; 9) | (0; 0) | (0; 0) | (0; 0) | (0; 0) |
| | | | | | --PANDAOPT-- | | |
| 7 | 1.613E+01 | ALMOST FEASIBLE | (0; 8) | (0; 0) | (0; 0) | (0; 0) | (0; 0) |
| 8 | 1.619E+01 | FEASIBLE | (0; 8) | (0; 0) | (0; 0) | (0; 0) | (0; 0) |
| | | | | | --PANDAOPT-- | | |
| 9 | 1.619E+01 | FEASIBLE | (0; 8) | (0; 0) | (0; 0) | (0; 0)<--optimum |

Initial face sheet waviness, w0/L = 0.001 and with the constraint:
(face sheet wrinkling halfwavelength)/(1.732*s) > 2.0 turned ON

**Table 9** OPTIMIZATION OF PANEL WITH SOME INITIAL FACE SHEET WAVINESS:
1. Initial face sheet waviness, w0/L = 0.001;
2. (face sheet wrinkling halfwavelength)/(1.732*s) > 2.0
constraint condition turned ON

---

**PART 2:** Optimum design of panel, initial facesheet waviness, w0/L=0.001;
(face sheet wrinkling halfwavelength)/(1.732*s) > 2.0 constraint
condition turned ON.

**VALUES OF DESIGN VARIABLES CORRESPONDING TO ALMOST FEASIBLE DESIGN**

| VAR. STR./ SEG. | LAYER | CURRENT | |
|---|---|---|---|
| NO. RNG NO. | NO. | VALUE | DEFINITION |
| 1  SKN  1 | 1 | 2.084E-02 | T(1 )(SKN):thickness for layer index no.(1) |
| 2  SKN  1 | 2 | 5.774E-01 | T(2 )(SKN):thickness for layer index no.(2) |
| 3  SKN  1 | 3 | 2.084E-02 | T(3 )(SKN):thickness for layer index no.(3) |
| 4  SKN  1 | 0 | 5.709E-02 | s(2 )(SKN):Length of one side of the hexagon |
| 5  SKN  1 | 0 | 8.920E-04 | tc(2 )(SKN):thickness of honeycomb cell wall |

**CORRESPONDING VALUE OF THE OBJECTIVE FUNCTION:**

| VAR. STR./ SEG. | LAYER | CURRENT | |
|---|---|---|---|
| NO. RNG NO. | NO. | VALUE | DEFINITION |

```
                0   0   1.612E+01   WEIGHT OF THE ENTIRE PANEL
----------------------------------------------------------------------
PART 3: Margins after optimization; Initial facesheet waviness, w0/L=0.001;
        (face sheet wrinkling halfwavelength)/(1.732*s) > 2.0 constraint
        condition turned ON;

BUCKLING LOAD FACTORS FOR LOCAL BUCKLING FROM KOITER v. BOSOR4 THEORY:
  Local buckling load factor from KOITER theory = 1.1814E+00
  Local buckling load factor from BOSOR4 theory = 1.1065E+00

MARGINS FOR CURRENT DESIGN: LOAD CASE NO. 1, SUBCASE NO. 1
MAR.  MARGIN
NO.   VALUE      DEFINITION
 1  5.90E-03  Local buckling from discrete model-1.,M=5  axial halfwaves;FS=1.1
 2  7.40E-02  Local buckling from Koiter theory,M=5    axial halfwaves;FS=1.1
 3  2.31E-03  eff.stress:matl-1,SKN,Dseg=2,node-11,layer=3,z=0.3096;x=0.3096; MID.;FS=1.
 4  2.77E-03  eff.stress:matl-1,SKN,Iseg=1,allnode,layer=3,z=0.3096;-MID.;FS=1.
 5  9.26E-03  buck.(DONL);simp-support general buck;M=5;M=1;slope=0.;FS=1.
 6  4.81E-02  localbuck (VINSON);strng Iseg1 ;MID; local buck.; M=5;FS=1.1
 7  1.64E+00  wrinkling ;strng Iseg1 ; MID;face 1; M=490;M=1;slope=0.;FS=1.
 8  2.39E-03  Facel wavelength/celldiam;STR;Iseg=1 ,Matl=2 ;MIDLENGTH;FS=1.
 9  1.51E+00  wrinkling ( HOFF );strng Iseg1 ; MID;face 1; M=491;FS=1.
10  4.42E+00  corecrimp (VINSON);strng Iseg1 ;MID; core crimping;FS=1.
11  1.13E+01  dimpling ;strng Iseg1 ; MID;face 1; M=1;M=1;slope=0.;FS=1.
12  1.64E+00  wrinkling ;strng Iseg1 ; MID;face 2; M=490;M=1;slope=0.;FS=1.
13  2.41E-03  Face2 wavelength/celldiam;STR;Iseg=1 ,Matl=2 ;MIDLENGTH;FS=1.
14  1.51E+00  wrinkling ( HOFF );strng Iseg1 ; MID;face 2; M=491;FS=1.
15  1.13E-01  dimpling ;strng Iseg1 ; MID;face 2; M=1;M=1;slope=0.;FS=1.
16  6.70E-04  Core crushing margin;STR;Iseg=1 ;Matl 2 ;MIDLENGTH;FS=1.
17  1.81E+00  L-dir. sandwich core shear;STR;Iseg=1 ;Matl 2 ;MIDLENGTH;FS=1.
18  3.09E+02  W-dir. sandwich core shear;STR;Iseg=1 ;Matl 2 ;MIDLENGTH;FS=1.
19  2.55E+00  face sheet pull-off margin;STR;Iseg=1 ;Matl 2 ;MIDLENGTH;FS=1.
20  1.44E+02  (Max.allowable ave.axial strain)/(ave.axial strain) -1; FS=1.
21  9.26E-03  buck.(SAND);simp-support general buck;M=5;M=1;slope=0.;FS=1.1
```

Table 10 Five margins computed in PANDA2 which, for the special case of the unstiffened flat panel, denote the same phenomenon: Overall panel buckling. This table is analogous to Tables 4 and 7.

```
 1  5.90E-03  Local buckling from discrete model-1.,M=5  axial halfwaves;FS=1.1
 2  7.40E-02  Local buckling from Koiter theory,M=5    axial halfwaves;FS=1.1
 5  9.26E-03  buck.(DONL);simp-support general buck;M=5;M=1;slope=0.;FS=1.1
 6  4.81E-02  localbuck (VINSON);strng Iseg1 ;MID; local buck.;M=5;FS=1.1
21  9.26E-03  buck.(SAND);simp-support general buck;M=5;M=1;slope=0.;FS=1.1
```

Table 11 OPTIMIZATION OF PANEL WITH w0/L = 0.001 AND EQ.(13) TURNED OFF:
1. Initial face sheet waviness, w0/L = 0.001;
2. (face sheet wrinkling halfwavelength)/(1.732*s) > 2.0 constraint condition turned OFF

```
PART 1: Optimum design of panel, Initial facesheet waviness, w0/L=0.001;
        (face sheet wrinkling halfwavelength)/(1.732*s) > 2.0 constraint
        condition turned OFF.
VALUES OF DESIGN VARIABLES CORRESPONDING TO FEASIBLE DESIGN
VAR. STR/ SEG. LAYER CURRENT
NO.  RNG  NO.   NO.   VALUE       DEFINITION
 1   SKN   1     1   2.084E-02  T(1 )(SKN):thickness for layer index no.(1)
 2   SKN   1     2   5.760E-01  T(2 )(SKN):thickness for layer index no.(2)
 3   SKN   1     3   2.084E-02  T(3 )(SKN):thickness for layer index no.(3)
 4   SKN   1     0   2.069E-01  s(2 )(SKN):Length of one side of the hexagon
 5   SKN   1     0   3.289E-03  tc(2 )(SKN):thickness of honeycomb cell wall
```

```
CURRENT VALUE OF THE OBJECTIVE FUNCTION:
VAR. STR/ SEG. LAYER CURRENT
NO.  RNG  NO.   NO.   VALUE       DEFINITION
 0    0              1.616E+01   WEIGHT OF THE ENTIRE PANEL

PART 2: Warning issued by PANDA2 when the constraint
        (face sheet wrinkling halfwavelength)/(1.732*s) > 2.0
        is badly violated.
***** WARNING Iseg= 1, Iloop= 1: ******
Facel wrinkle halfwavelength is less than the honeycomb cell diameter.
(face1 wrinkle halfwavelength)/(cell diameter)= 5.6723E-01
***** WARNING Iseg= 1, Iloop= 1: ******
Face2 wrinkle halfwavelength is less than the honeycomb cell diameter.
(face2 wrinkle halfwavelength)/(cell diameter)= 5.6725E-01

PART 3: Margins after optimization; initial facesheet waviness, w0/L=0.001;
        (face sheet wrinkling halfwavelength)/(1.732*s) > 2.0 constraint
        condition turned OFF.

MARGINS FOR CURRENT DESIGN: LOAD CASE NO. 1, SUBCASE NO. 1
MAR.  MARGIN
NO.   VALUE      DEFINITION
 1 -5.27E-05  Local buckling from discrete model-1.,M=5  axial halfwaves;FS=1.1
 2  6.72E-02  Local buckling from Koiter theory,M=5    axial halfwaves;FS=1.1
 3 -1.97E-04  eff.stress:matl-1,SKN,Dseg=2,node-11,layer=3,z=0.3088; MID.;FS=1.
 4  2.91E-04  eff.stress:matl-1,SKN,Iseg=1,allnode,layer=3,z=0.3088;-MID.;FS=1.
 5  3.30E-03  buck.(DONL);simp-support general buck;M=5;M=1;slope=0.;FS=1.1
 6  4.16E-02  localbuck (VINSON);strng Iseg1 ;MID; local buck.; M=5;FS=1.1
 7  1.62E+00  wrinkling ;strng Iseg1 ; MID;face 1; M=490;M=1;slope=0.;FS=1.
 8  1.50E+00  wrinkling ( HOFF );strng Iseg1 ; MID;face 1; M=492;FS=1.
 9  4.42E+00  corecrimp (VINSON);strng Iseg1 ;MID; core crimping;FS=1.
10  2.91E-01  dimpling ;strng Iseg1 ; MID;face 1; M=1;M=1;slope=0.;FS=1.
11  1.62E+00  wrinkling ;strng Iseg1 ; MID;face 2; M=490;M=1;slope=0.;FS=1.
12  1.50E+00  wrinkling ( HOFF );strng Iseg1 ; MID;face 2; M=492;FS=1.
13  2.91E-01  dimpling ;strng Iseg1 ; MID;face 2; M=1;M=1;slope=0.;FS=1.
14  6.25E-04  Core crushing margin;STR;Iseg=1 ;Matl 2 ;MIDLENGTH;FS=1.
15  1.79E+02  L-dir. sandwich core shear;STR;Iseg=1 ;Matl 2 ;MIDLENGTH;FS=1.
16  2.93E+02  W-dir. sandwich core shear;STR;Iseg=1 ;Matl 2 ;MIDLENGTH;FS=1.
17 -1.63E-04  face sheet pull-off margin;STR;Iseg=1 ;Matl 2 ;MIDLENGTH;FS=1.
18  1.44E+02  (Max.allowable ave.axial strain)/(ave.axial strain) -1; FS=1.
19  3.30E-03  buck.(SAND);simp-support general buck;M=5;M=1;slope=0.;FS=1.1
```

Table 12 Comparison of certain results from Tables 9 and 11, which correspond to two different optimum designs found with PANDA2. The two different optima are essentially the same design except for "s", the hexagonal cell side width, and "tc" the cell wall thickness. The ratio, s/tc, is approximately the same for both optima.

```
From Table 9  (Eq.(13) turned ON):  optimized "s" and "tc" and certain margins:
 4  SKN  1  0  5.709E-02  s(2 )(SKN):Length of one side of the hexagon
 5  SKN  1  0  8.920E-04  tc(2 )(SKN):thickness of honeycomb cell wall
11  SKN  1     1.13E+01  dimpling ;strng Iseg1 ; MID;face 1; M=1;M=1;slope=0.;FS=1.
15  SKN  1     1.13E+01  dimpling ;strng Iseg1 ; MID;face 2; M=1;M=1;slope=0.;FS=1.
19  SKN  1     2.55E+00  face sheet pull-off margin;STR;Iseg=1 ;Matl 2 ;MIDLENGTH;FS=1.

From Table 11 (Eq.(13) turned OFF): optimized "s" and "tc" and certain margins:
 4  SKN  1  0  2.069E-01  s(2 )(SKN):Length of one side of the hexagon
 5  SKN  1  0  3.289E-03  tc(2 )(SKN):thickness of honeycomb cell wall
10  SKN  1     2.91E-01  dimpling ;strng Iseg1 ; MID;face 1; M=1;M=1;slope=0.;FS=1.
13  SKN  1     2.91E-01  dimpling ;strng Iseg1 ; MID;face 2; M=1;M=1;slope=0.;FS=1.
17  SKN  1    -1.63E-04  face sheet pull-off margin;STR;Iseg=1 ;Matl 2 ;MIDLENGTH;FS=1.
```

Table 13   Margins for IMPERFECT panel with same dimensions as the optimized "perfect" panel. Buckling modal imperfection amplitude, W0=0.1 in. t(face)=0.02084, t(core)=0.5774, s=0.05709, tc=0.000892 in.
1. Initial face sheet waviness, w0/L = 0.001;
2. (face sheet wrinkling halfwavelength)/(1.732*s) > 2.0 constraint condition turned ON
3. Buckling modal imperfection amplitude, W0 = 0.1 in.

MARGINS FOR CURRENT DESIGN: LOAD CASE NO. 1, SUBCASE NO. 1

| MAX. MARGIN | | |
|---|---|---|
| NO. | VALUE | DEFINITION |

Table 14   Facesheet resultants in the "perfect" and imperfect sandwich panel. Buckling modal imperfection amplitude, W0 = 0.1 in; Initial face sheet waviness, w0/L = 0.001 t(face)=0.02084, t(core)=0.5774, s=0.05709, tc=0.000892 in.

FORCE RESULTANTS IN SANDWICH FACESHEETS FROM KOITER THEORY (SUB. STRTNK) ASSUMED TO BE UNIFORM OVER SKIN-STRINGER MODULE SEGMENTS, USED FOR CONSTRAINTS

## Right column listing

| No. | | Value | Description |
|---|---|---|---|
| 1 | 1 | 8.48E-01 | Local buckling from discrete model-1.;M=5 axial halfwaves;FS=1.1 |
| 2 | 1 | 1.02E+00 | Local buckling from Koiter theory;M=5 axial halfwaves;FS=1.1 |
| 3 | 1 | 1.77E-02 | eff.stress:matl-1,SKN.Dseg=2;node=11,layer=3;x=0.4078; MID.;FS=1. |
| 4 | 1 | -3.60E-03 | eff.stress:matl-1,SKN.Iseg=1,allnode,layer=1;x=0.4078;-MID.;FS=1. |
| 5 | 1 | 8.54E-01 | buck.(DOML);simp-support general buck;M=5;M=1;slope=0.;FS=1.1 |
| 6 | 1 | 9.62E-01 | localbuck (VIMBOM);strng Iseg1 ;MID; local buck.; M=5;FS=1.1 |
| 7 | 1 | 1.34E+00 | wrinkling ;strng Iseg1 ; MID;face 1; M=417;M=2;slope=0.132;FS=1. |
| 8 | 1 | 6.19E-04 | Facel wavelength/celldiam;STR;Iseg-1 ;Matl-2 ;MIDLENGTH;FS=1. |
| 9 | 1 | 1.39E+00 | wrinkling ( MOF )strng Iseg1 ; MID;face 1; M=450;FS=1. |
| 10 | 1 | 4.90E+00 | corecrimp (VIMSOM);strng Iseg1 ;MID; core crimping;FS=1. |
| 11 | 1 | 9.37E+00 | dimpling ;strng Iseg1 ; MID;face 1; M=1;M=1;slope=0.05;FS=1. |
| 12 | 1 | 1.34E+00 | wrinkling ;strng Iseg1 ; MID;face 2; M=417;M=2;slope=0.132;FS=1. |
| 13 | 1 | 6.19E-04 | Face2 wavelength/celldiam;STR;Iseg-1 ;Matl-2 ;MIDLENGTH;FS=1. |
| 14 | 1 | 1.39E+00 | wrinkling ( MOF )strng Iseg1 ; MID;face 2; M=450;FS=1. |
| 15 | 1 | 9.37E+00 | dimpling ;strng Iseg1 ; MID;face 2; M=1;M=1;slope=0.05;FS=1. |
| 16 | 1 | -1.33E-02 | Core crushing margin;STR;Iseg=1 ;Matl 2 ;MIDLENGTH;FS=1. |
| 17 | 1 | 1.78E-01 | L-dir. sandwich core shear;STR;Iseg-1 ;Matl 2 ;MIDLENGTH;FS=1. |
| 18 | 1 | 3.77E-01 | W-dir. sandwich core shear;STR;Iseg-1 ;Matl 2 ;MIDLENGTH;FS=1. |
| 19 | 1 | 1.58E+00 | face sheet pull-off ave.axial strain;STR;Iseg=1 ;Matl 2 ;MIDLENGTH;FS=1. |
| 20 | 1 | 1.61E+02 | (Max.allowable ave.axial strain) -1;FS=1. |
| 21 | 1 | 8.54E-01 | buck.(SAND);simp-support general buck;M=5;M=1;slope=0.;FS=1.1 |

**Table 16** Effect of temperature gradient through the thickness:
1. Initial face sheet waviness, w0/L = 0.001;
2. (face sheet wrinkling halfwavelength)/(1.732*s) > 2.0
   constraint condition turned ON
3. Amplitude of the buckling modal imperfection, W0 = 0.1 in.
   t(face)=0.02379, t(core)=0.7453, s=0.06464, tc=0.001133 in.
   is the optimum found with zero temperature gradient.

| | | |
|---|---|---|
| | y | $ Is there any thermal "loading" in this load set? |
| bottom face --> | 400 | $ Temperature rise, panel skin, surface opposite stringer |
| top face --> | 000 | $ Temperature rise, panel skin, upper surface |
| | n | $ Is the thermal loading part of Load Set B? |

================================================

**PART 1**

FORCE RESULTANTS IN SANDWICH FACESHEETS AFTER CALL TO SUB. STACON
(IMPERFECT PANEL, NO THERMAL GRADIENT THROUGH PANEL THICKNESS)

Segment  Top (or leftmost) facesheet 1         Bottom (or rightmost) facesheet 2
Iseg   Axial, Mx  Hoop, My  Shear, Mxy      Axial, Mx  Hoop, My  Shear, Mxy
SKM 1 -3.1111E+03 -5.9808E+02 3.3798E+02 -3.1111E+03 -5.9808E+02 3.3798E+02

**PART 2**

FORCE RESULTANTS IN SANDWICH FACESHEETS AFTER CALL TO SUB. STACON
(IMPERFECT PANEL, INCLUDING THERMAL GRADIENT THROUGH PANEL THICKNESS)

Segment  Top (or leftmost) facesheet 1         Bottom (or rightmost) facesheet 2
Iseg   Axial, Mx  Hoop, My  Shear, Mxy      Axial, Mx  Hoop, My  Shear, Mxy
SKM 1 -2.4078E+03 -3.6908E+02 3.3798E+02 -3.8144E+03 -8.2707E+02 3.3798E+02

**PART 3**  Margins INCLUDING thermal gradient. Design is the optimum design
found with no thermal gradient, imperfect panel: PART 2, Table 271.15
t(face)=0.02379, t(core)=0.7453, s=0.06464, tc=0.001133 in.
MARGINS FOR CURRENT DESIGN: LOAD CASE NO. 1, SUBCASE NO. 1
MAR. MARGIN
NO. VALUE

| No. | | Value | Description |
|---|---|---|---|
| 1 | 1 | 7.64E-01 | Local buckling from discrete model-1.;M=5 axial halfwaves;FS=1.1 |
| 2 | 1 | 9.25E-01 | Local buckling from Koiter theory;M=5 axial halfwaves;FS=1.1 |
| 3 | 1 | -1.70E-01 | eff.stress:matl-1,SKN.Dseg=2;node=11,layer=3;x=0.3964; MID.;FS=1. |
| 4 | 1 | -1.86E-01 | eff.stress:matl-1,SKN.Iseg=1,allnode,layer=3;x=0.3964;-MID.;FS=1. |
| 5 | 1 | 7.70E-01 | buck.(DOML);simp-support general buck;M=5;M=1;slope=0.;FS=1.1 |
| 6 | 1 | 8.71E-01 | localbuck (VIMSOM);strng Iseg1 ;MID; local buck.; M=5;FS=1.1 |
| 7 | 1 | 2.02E+00 | wrinkling ;strng Iseg1 ; MID;face 1; M=418;M=2;slope=0.1757;FS=1. |
| 8 | 1 | 1.15E-03 | Facel wavelength/celldiam;STR;Iseg-1 ;Matl-2 ;MIDLENGTH;FS=1. |
| 9 | 1 | 2.06E+00 | wrinkling ( MOF )strng Iseg1 ; MID;face 1; M=446;FS=1. |
| 10 | 1 | 4.54E+00 | corecrimp (VIMSOM);strng Iseg1 ;MID; core crimping;FS=1. |
| 11 | 1 | 1.25E+01 | dimpling ;strng Iseg1 ; MID;face 1; M=1;M=1;slope=0.06;FS=1. |

## Left column

| No. | | Value | | Value |
|---|---|---|---|---|
| 1, | 1 | 6.3017E+02 | | 2.3818E-01 |
| 1, | 2 | 6.2321E+02 | | 6.4027E-01 |
| 1, | 3 | 6.0234E+02 | | 1.5305E+02 |
| 1, | 4 | 5.6759E+02 | | 2.4217E+02 |
| 1, | 5 | 5.1911E+02 | | 3.3007E+02 |
| 1, | 6 | 4.5735E+02 | | 4.1444E+02 |
| 1, | 7 | 3.8319E+02 | | 4.9202E+02 |
| 1, | 8 | 2.9807E+02 | | 5.5903E+02 |
| 1, | 9 | 2.0402E+02 | | 6.1154E+02 |
| 1, | 10 | 1.0365E+02 | | 6.4621E+02 |
| 1, | 11 | 1.1774E-07 | | 6.6068E+02 |
| 2, | 1 | 1.1775E-07 | | 6.6856E+02 |
| 2, | 2 | 1.0365E+02 | | 5.5408E+02 |
| 2, | 3 | 2.0402E+02 | | 6.2707E+02 |
| 2, | 4 | 2.9807E+02 | | 5.8175E+02 |
| 2, | 5 | 3.8319E+02 | | 5.2133E+02 |
| 2, | 6 | 4.5735E+02 | | 4.4951E+02 |
| 2, | 7 | 5.1911E+02 | | 3.7001E+02 |
| 2, | 8 | 5.6759E+02 | | 2.8595E+02 |
| 2, | 9 | 6.0234E+02 | | 1.9962E+02 |
| 2, | 10 | 6.2321E+02 | | 1.1229E+02 |
| 2, | 11 | 6.3017E+02 | | 2.4403E-01 |

**PART 5b:** "worst" values; used by PANDA2 to build x-x ('L'-direction) and
y-x ('W'-direction) sandwich core transverse shear constraints
and deformation-induced core crushing constraint
DEFORMATION-INDUCED PRESSURE TENDING TO
CRUSH THE CORE (COMPUTED IN SUB. STATNK) AND MAXIMUM
TRANSVERSE SHEAR STRESSES (COMPUTED IN SUB. STRMID)
ON THE "X" AND "Y" SIDES OF THE SANDWICH CORE

| Segment | Crushing | X-transverse | Y-transverse |
|---|---|---|---|
| Iseg | pressure | shear stress | shear stress |
| SKM 1 | 9.3920E+01 | 6.3017E+02 | 6.6856E+02 |

================================================

**Table 15** Optimization of IMPERFECT Titanium/Aluminum Sandwich Panel
Amplitude of the buckling modal imperfection, w0 = 0.1 in.
1. Initial face sheet waviness, w0/L = 0.001;
2. (face sheet wrinkling halfwavelength)/(1.732*s) > 2.0
   constraint condition turned ON
3. Buckling modal imperfection amplitude, W0 = 0.1 in.

================================================

**PART 1:** Optimization (omitted here to save space. See Table 271.15 in
ITEM 271 of [29])

================================================

**PART 2** Optimum design, IMPERFECT panel
VALUES OF DESIGN VARIABLES CORRESPONDING TO ALMOST FEASIBLE DESIGN

| VAR. NO. | STR./ RNG NO. | SEG. NO. | LAYER NO. | CURRENT VALUE | | DEFINITION |
|---|---|---|---|---|---|---|
| 1 | SKM | 1 | 1 | 2.379E-02 | T(1 )(SKM):thickness for layer index no.(1) |
| 2 | SKM | 1 | 2 | 7.453E-01 | T(2 )(SKM):thickness for layer index no.(2) |
| 3 | SKM | 1 | 3 | 2.379E-02 | T(3 )(SKM):thickness for layer index no.(3) |
| 4 | SKM | 1 | 0 | 6.464E-02 | s(2 )(SKM):Length of one side of the hexagon |
| 5 | SKM | 1 | 0 | 1.133E-03 | tc(2 )(SKM):thickness of honeycomb cell wall |

================================================

**PART 3** Objective, IMPERFECT panel
CORRESPONDING VALUE OF THE OBJECTIVE FUNCTION:

| VAR. NO. | STR./ RNG NO. | SEG. LAYER NO. | CURRENT VALUE | | DEFINITION |
|---|---|---|---|---|---|
| 0 | 0 | 0 | 1.925E+01 | WEIGHT OF THE ENTIRE PANEL |

================================================

**PART 4** Margins at the optimum design, IMPERFECT panel
MARGINS FOR CURRENT DESIGN: LOAD CASE NO. 1, SUBCASE NO. 1
MAR. MARGIN
NO. VALUE                DEFINITION

| 12 | 9.29E-01 | wrinkling ;strng Iseg1 ; MID;face 2; M=417;M=2;slope=0.11;FS=1. |
|---|---|---|
| 13 | 1.15E-03 | Face2 wavelength/celldim;STR;Iseg=1 ;Matl=2 ;MIDLENGTH;FS=1. |
| 14 | 9.10E-01 | wrinkling ( HOFF );strng Iseg1 ; MID;face 2; M=446;FS=1. |
| 15 | 7.18E+00 | dimpling ;strng Iseg1 ; MID;face 2; M=1;M=1;slope=0.04;FS=1. |
| 16 | -3.48E-01 | Core crushing margin;STR,Iseg=1 ;Matl 2 ;MIDLENGTH;FS=1. |
| 17 | -6.61E-02 | L-dir. sandwich core shear;STR;Iseg=1 ;Matl 2 ;MIDLENGTH;FS=1. |
| 18 | 2.43E-01 | W-dir. sandwich core shear;STR;Iseg=1 ;Matl 2 ;MIDLENGTH;FS=1. |
| 19 | 7.53E-01 | face sheet pull-off margin;STR;Iseg=1 ;Matl 2 ;MIDLENGTH;FS=1. |
| 20 | 1.62E+02 | (Max.allowable ave.axial strain)/(ave.axial strain) -1; FS=1. |
| 21 | 7.70E-01 | buck.(SAND);simp-support general buck;M=5;M=1;slope=0.;FS=1.1 |

**Table 17**    Optimization of IMPERFECT Titanium/Aluminum Sandwich Panel
WITH through-thickness temperature gradient as specified
in the heading of Table 271.16.
1. Initial face sheet waviness, w0/L = 0.001;
2. (face sheet wrinkling halfwavelength)/(1.732*s) > 2.0
   constraint condition turned ON
3. Amplitude of the buckling model imperfection, W0 = 0.1 in.
Starting design:
t(face)=0.02379, t(core)=0.7453, s=0.06464, tc=0.001133 in.
is the optimum found with zero temperature gradient.
Bottom face sheet HOT.

**PART 1:** Optimization (omitted here to save space. See Table 271.17 in
ITEM 271 of [29])

**PART 2** Optimum design with buckling model imperfection (W0=0.1 in.) plus
thermal gradient as specified in the heading of Table 16:
bottom face sheet HOT.

| VAR. NO. | STR/ RNG | SEG. NO. | LAYER NO. | CURRENT VALUE | DEFINITION |
|---|---|---|---|---|---|
| 1 | SKN | 1 | 1 | 1.485E-02 | T(1 )(SKN):thickness for layer index no.(1) |
| 2 | SKN | 1 | 2 | 7.778E-01 | T(2 )(SKN):thickness for layer index no.(2) |
| 3 | SKN | 1 | 3 | 3.780E-02 | T(3 )(SKN):thickness for layer index no.(3) |
| 4 | SKN | 1 | 0 | 4.061E-02 | s(2 )(SKN):Length of one side of the hexagon |
| 5 | SKN | 1 | 0 | 7.000E-04 | tc(2 )(SKN):thickness of honeycomb cell wall |

**PART 3** Objective, IMPERFECT panel WITH thermal gradient
CORRESPONDING VALUE OF THE OBJECTIVE FUNCTION:

| VAR. NO. | STR/ RNG | SEG. NO. | LAYER NO. | CURRENT VALUE | DEFINITION |
|---|---|---|---|---|---|
| 0 | 0 | 0 | 0 | 2.098E+01 | WEIGHT OF THE ENTIRE PANEL |

**PART 4** Margins at the optimum design, IMPERFECT panel WITH thermal gradient
Bottom face sheet HOT

**BUCKLING LOAD FACTORS FOR CURRENT DESIGN: LOAD CASE NO. 1, SUBCASE NO. 1**
Local buckling load factor from KOITER theory = 2.0947E+00
Local buckling load factor from BOSOR4 theory = 1.9288E+00

**MARGINS FOR CURRENT DESIGN: LOAD CASE NO. 1, SUBCASE NO. 1**

| MAR. NO. | MARGIN VALUE | DEFINITION |
|---|---|---|
| 1 | 7.53E-01 | Local buckling from discrete model-1.,M=5    axial halfwaves;FS=1.1 |
| 2 | 9.04E-01 | Local buckling from Koiter theory;M=5    axial halfwaves;FS=1.1 |
| 3 | 2.13E-02 | eff.stress:matl=1,SKN,Dseg=2,node=11,layer=3,x=0.2457; MID.;FS=1. |
| 4 | -6.42E-04 | eff.stress:matl=1.SKN,Iseg=1,allnode,layer=3,x=0.2457;-MID.;FS=1. |
| 5 | 7.59E-01 | buck.(DOME);simp-support general buck;M=5;M=1;slope=0.;FS=1. |
| 6 | 8.52E-01 | localbuck (VINSON);strng Iseg1 ;MID; local buck.; M=5;FS=1.1 |
| 7 | 1.48E+00 | wrinkling ;strng Iseg1 ; MID;face 1; M=595;M=1;slope=0.2737;FS=1. |
| 8 | -1.45E-04 | Face1 wavelength/celldim;STR;Iseg=1 ;Matl=2 ;MIDLENGTH;FS=1. |
| 9 | 1.61E+00 | wrinkling (VINSON);strng Iseg1 ; MID;face 1; M=711;FS=1. |
| 10 | 4.79E+00 | corecrimp (VINSON);strng Iseg1 ;MID; core crimping;FS=1. |
| 11 | 1.24E+01 | dimpling ;strng Iseg1 ; MID;face 1; M=1;M=1;slope=0.0917;FS=1. |
| 12 | 1.96E+00 | wrinkling ;strng Iseg1 ; MID;face 2; M=304;M=3;slope=0.0817;FS=1. |

| 13 | 1.55E+00 | Face2 wavelength/celldim;STR;Iseg=1 ;Matl=2 ;MIDLENGTH;FS=1. |
|---|---|---|
| 14 | 1.44E+00 | wrinkling ( HOFF );strng Iseg1 ; MID;face 2; M=279;FS=1. |
| 15 | 2.36E+01 | dimpling ;strng Iseg1 ; MID;face 2; M=1;M=1;slope=0.03;FS=1. |
| 16 | -2.45E-03 | Core crushing margin;STR,Iseg=1 ;Matl 2 ;MIDLENGTH;FS=1. |
| 17 | 1.75E-01 | L-dir. sandwich core shear;STR;Iseg=1 ;Matl 2 ;MIDLENGTH;FS=1. |
| 18 | 3.00E-01 | W-dir. sandwich core shear;STR;Iseg=1 ;Matl 2 ;MIDLENGTH;FS=1. |
| 19 | 3.39E+00 | sandwichcore tension margin;STR;Iseg=1 ;Matl 2 ;MIDLENGTH;FS=1. |
| 20 | 1.80E+02 | (Max.allowable ave.axial strain)/(ave.axial strain) -1; FS=1. |
| 21 | 7.59E-01 | buck.(SAND);simp-support general buck;M=5;M=1;slope=0.;FS=1.1 |

**Table 18**    Optimized designs for IMPERFECT panel WITH thermal gradient
obtained from SUPEROPT
(See [20] and panda2.news ITEMs 151,152,194, [29] for SUPEROPT)
Thermal gradient: temperature rise in one facesheet = 400 deg.
temperature rise in the other facesheet = 0.0 deg.
1. Initial face sheet waviness, w0/L = 0.001;
2. (face sheet wrinkling halfwavelength)/(1.732*s) > 2.0
   constraint condition turned ON
3. Amplitude of the buckling model imperfection, W0 = 0.1 in.
Starting design:
t(face)=0.02379, t(core)=0.7453, s=0.06464, tc=0.001133 in.
is the optimum found with zero temperature gradient.

**PART 1** Optimum design obtained from SUPEROPT for bottom facesheet
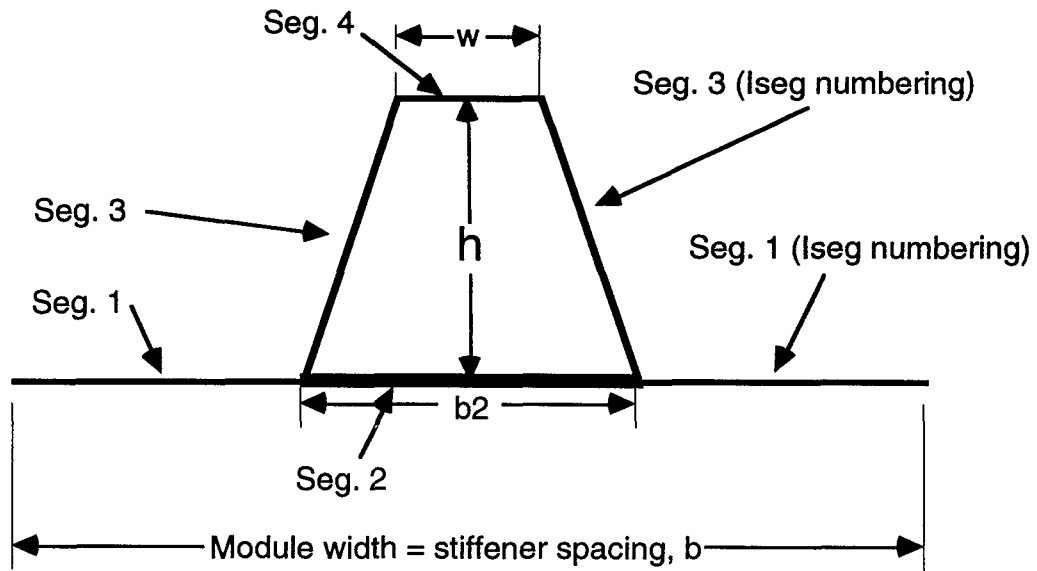temperature rise = 400 deg., top facesheet = 0 deg.
VALUES OF DESIGN VARIABLES CORRESPOND. TO ALMOST FEASIBLE DESIGN

| VAR. NO. | STR/ RNG | SEG. NO. | LAYER NO. | CURRENT VALUE | DEFINITION |
|---|---|---|---|---|---|
| 1 | SKN | 1 | 1 | 1.489E-02 | T(1 )(SKN):thickness for layer index no.(1) |
| 2 | SKN | 1 | 2 | 7.762E-01 | T(2 )(SKN):thickness for layer index no.(2) |
| 3 | SKN | 1 | 3 | 3.749E-02 | T(3 )(SKN):thickness for layer index no.(3) |
| 4 | SKN | 1 | 0 | 4.075E-02 | s(2 )(SKN):Length of one side of the hexagon |
| 5 | SKN | 1 | 0 | 2.088E+01 | tc(2 )(SKN):thickness of honeycomb cell wall |
| | | | | | WEIGHT OF THE ENTIRE PANEL |

**PART 2** Optimum design obtained from SUPEROPT for bottom facesheet
temperature rise = 0 deg., top facesheet = 400 deg.
VALUES OF DESIGN VARIABLES CORRESPOND. TO ALMOST FEASIBLE DESIGN

| VAR. NO. | STR/ RNG | SEG. NO. | LAYER NO. | CURRENT VALUE | DEFINITION |
|---|---|---|---|---|---|
| 1 | SKN | 1 | 1 | 3.802E-02 | T(1 )(SKN):thickness for layer index no.(1) |
| 2 | SKN | 1 | 2 | 7.431E-01 | T(2 )(SKN):thickness for layer index no.(2) |
| 3 | SKN | 1 | 3 | 1.480E-02 | T(3 )(SKN):thickness for layer index no.(3) |
| 4 | SKN | 1 | 0 | 4.023E-02 | s(2 )(SKN):Length of one side of the hexagon |
| 5 | SKN | 1 | 0 | 7.000E-04 | tc(2 )(SKN):thickness of honeycomb cell wall |
| | | | | 2.089E+01 | WEIGHT OF THE ENTIRE PANEL |

Segment numbering for single module model, "Iseg" numbering

## (a)
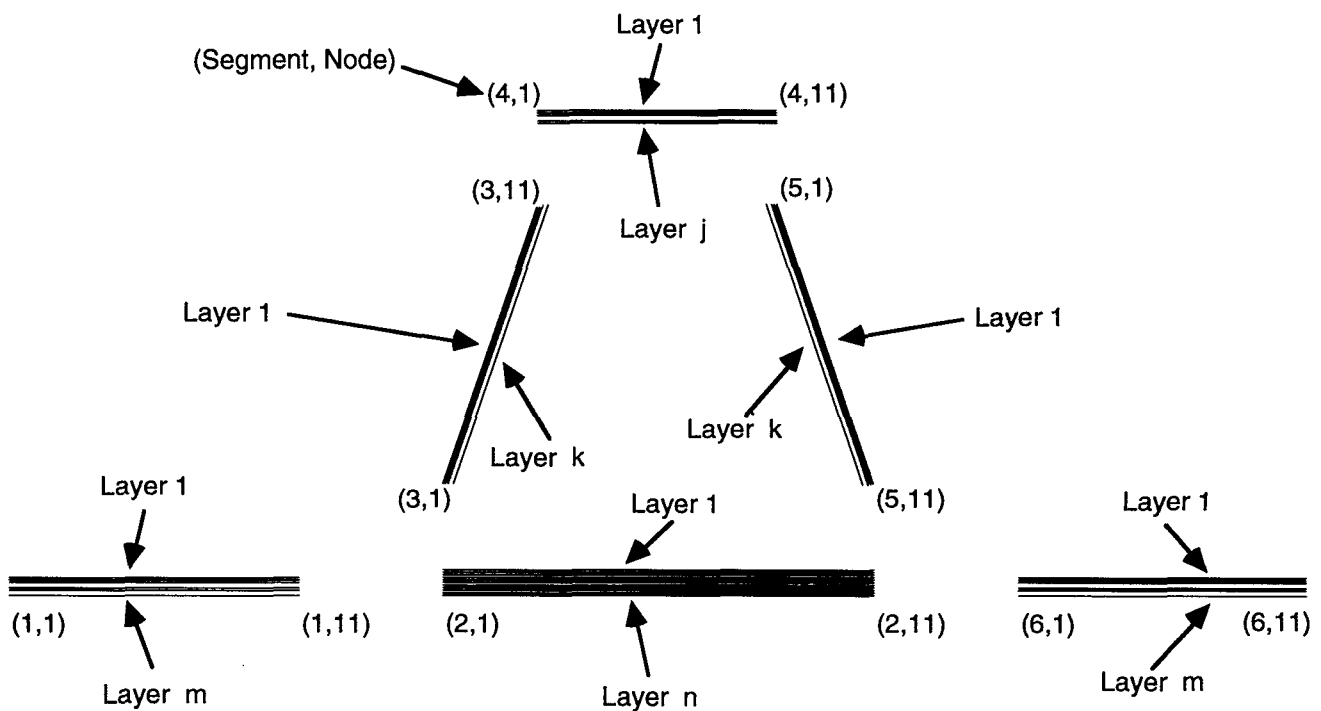
Segment numbering for single module model, "Dseg" numbering

## (b)

Fig. 1 Single module model of panel: (a) Numbering of module
segments for input data and PANDA type [21] models,
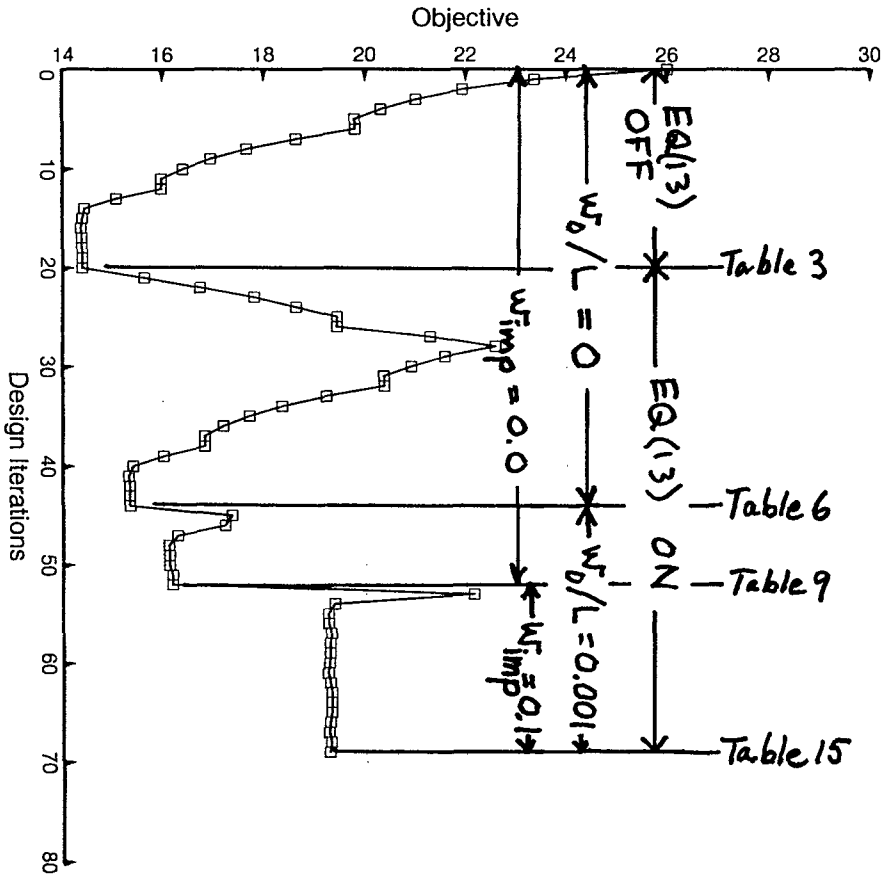(b) Segment numbering for discretized single module

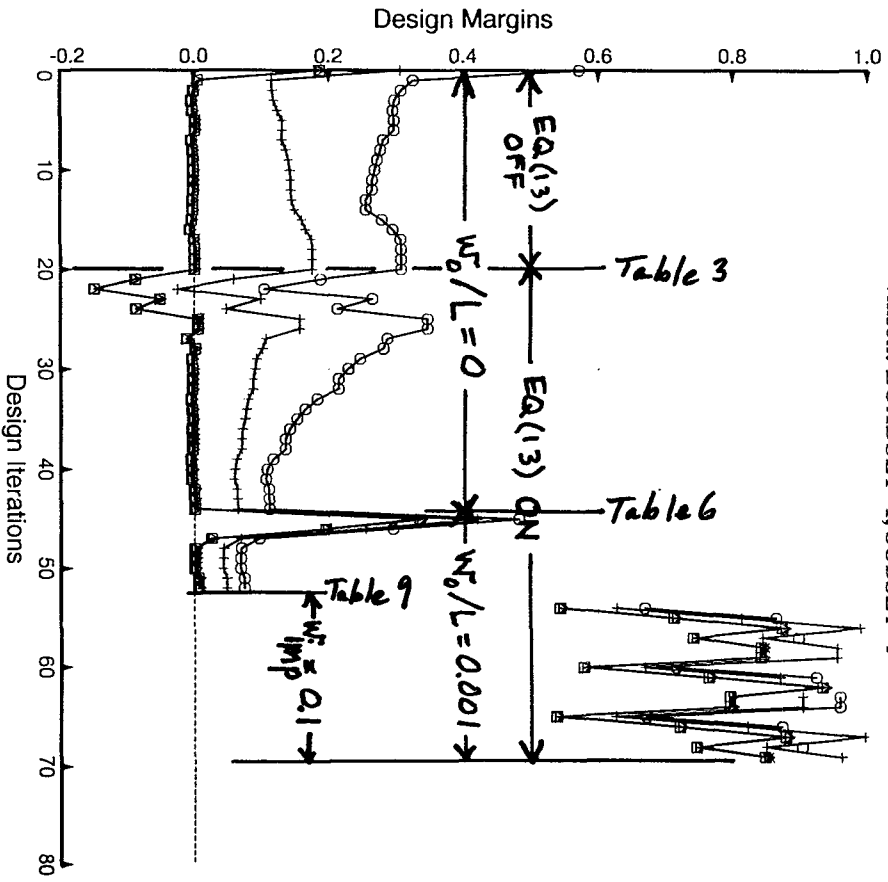Fig. 2 Panel weight during optimization cycles

□ WEIGHT OF THE ENTIRE PANEL.
vinson. SEE FILES vinson.OPM AND vinson.OPP



Fig. 3 The five margins that predict overall buckling of the unstiffened panel

□ 1 .1.1 Local buckling: discrete model
○ 2 .1.1 Local buckling: Koiter theory.
△ 5 .1.1 buck(DONL)simp-support general buck; MIDLENGTH
+ 6 .1.1 localbuck (VINSON);strng lseg1 local buck.; MIDLENGTH
× 12.1.1 buck(SAND)simp-support general buck; MIDLENGTH

vinson: LOADSET=1, SUBSET=1

2198

□  3 .1.1 eff.stress:matl=1; MID.
○  4 .1.1 eff.stress:matl=1,allnode;-MID.

□  7 .1.1 corecrimp (VINSON);strng lseg1  core crimping
○  17.1.1 Core crushing margin;STR;lseg=1 ;Matl 2
△  18.1.1 L-dir. sandwich core shear;STR;lseg=1 ;Matl 2
+  19.1.1 W-dir. sandwich core shear;STR;lseg=1 ;Matl 2

**vinson: LOADSET=1, SUBSET=1**

**vinson: LOADSET=1, SUBSET=1**



Fig. 4 Effective stress margins



Fig. 5 Margins for sandwich core crimping, crushing,
and L- and W-direction transverse shear stress
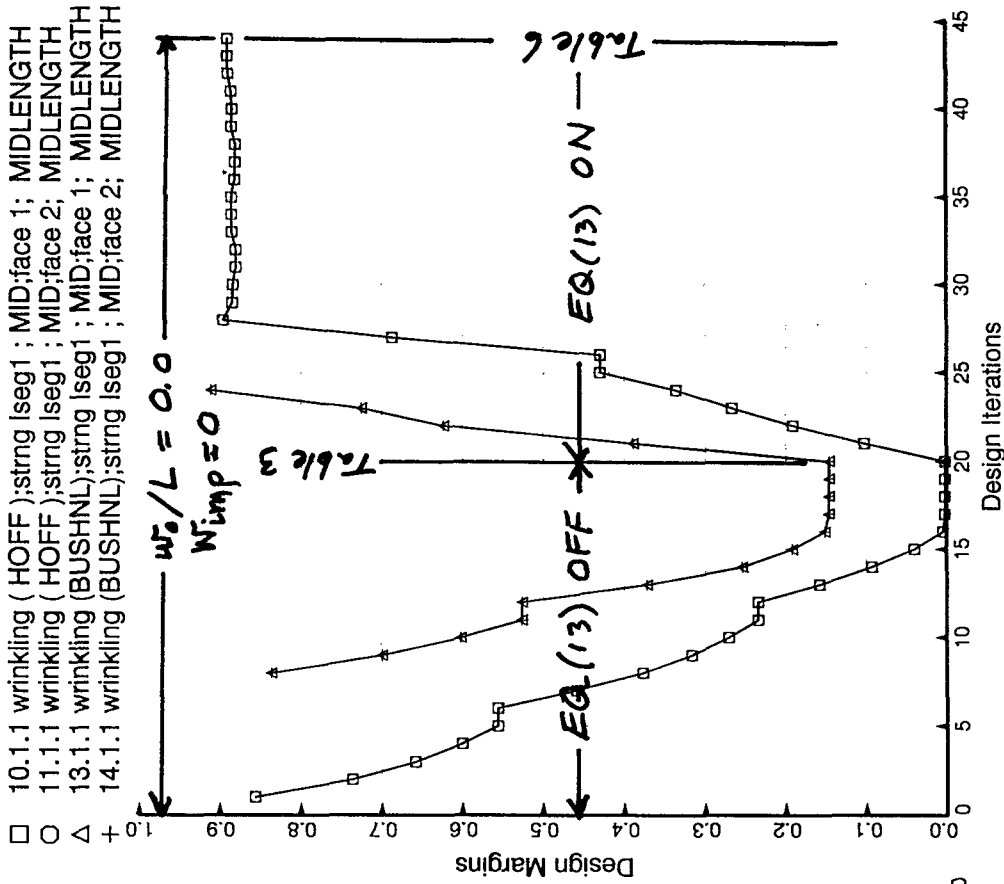
Fig. 7 Margins for face sheet wrinkling

□ 10.1.1 wrinkling (HOFF);strng lseg1 ; MID;face 1; MIDLENGTH
O 11.1.1 wrinkling (HOFF);strng lseg1 ; MID;face 2; MIDLENGTH
△ 13.1.1 wrinkling (BUSHNL);strng lseg1 ; MID;face 1; MIDLENGTH
+ 14.1.1 wrinkling (BUSHNL);strng lseg1 ; MID;face 2; MIDLENGTH
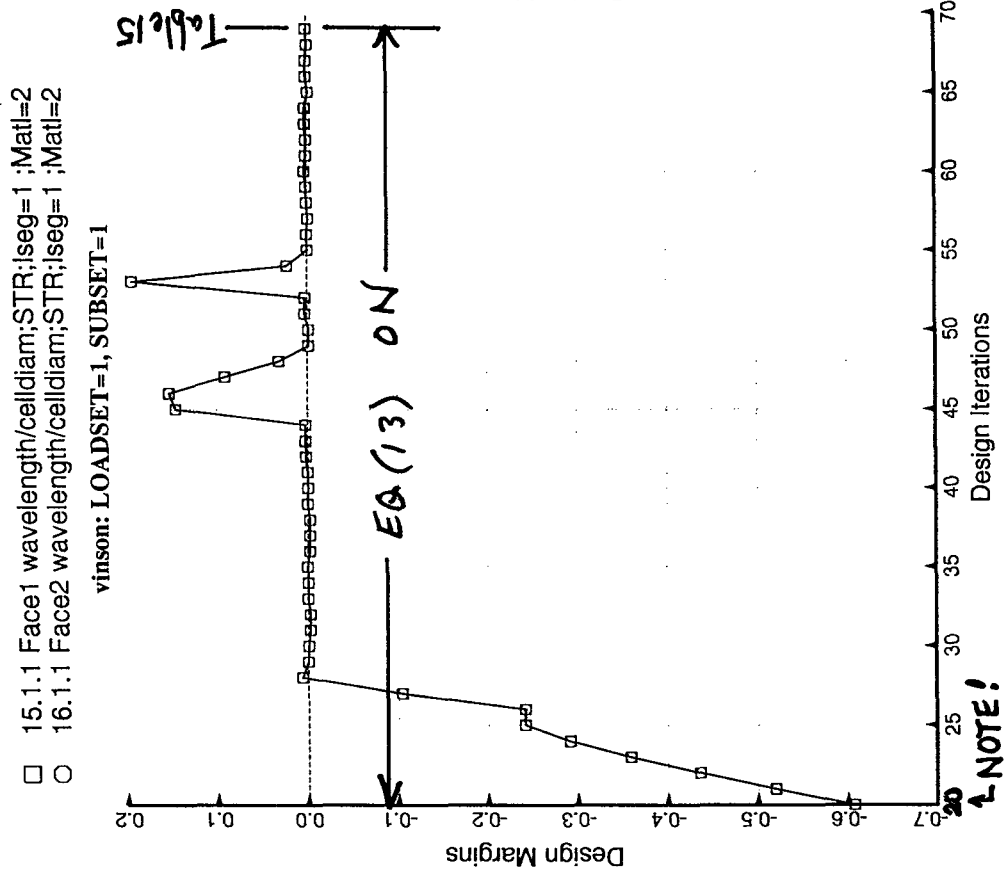


Fig. 6 Margins for honeycomb cell size constraint:
(face sheet wrinkling halfwavelength)/(1.732*s) > 2

□ 15.1.1 Face1 wavelength/celldiam;STR;lseg=1 ;Matl=2
O 16.1.1 Face2 wavelength/celldiam;STR;lseg=1 ;Matl=2

vinson: LOADSET=1, SUBSET=1
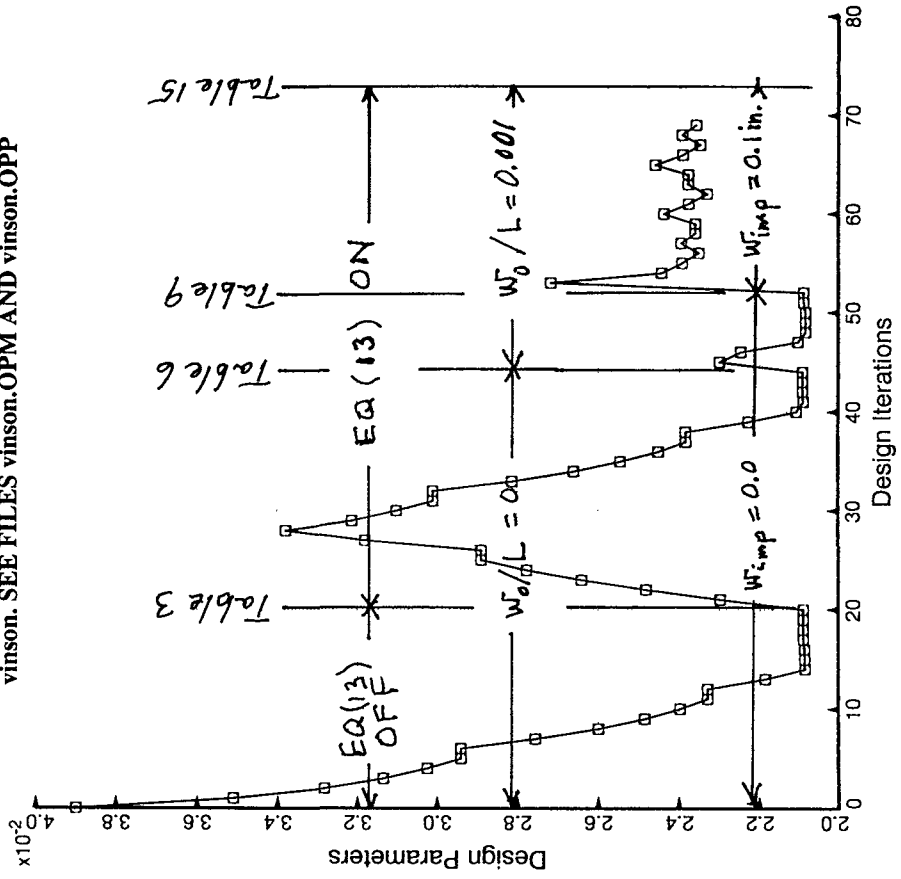
Fig. 9 Evolution of face sheet thickness



Fig. 8 Margins for face sheet dimpling

Design Parameters

T(2)(SKN):thickness for layer index no.(2): STR seg=1 , layer=2     s(2)(SKN):Length of one side of the hexagon, s(2): STR seg=1

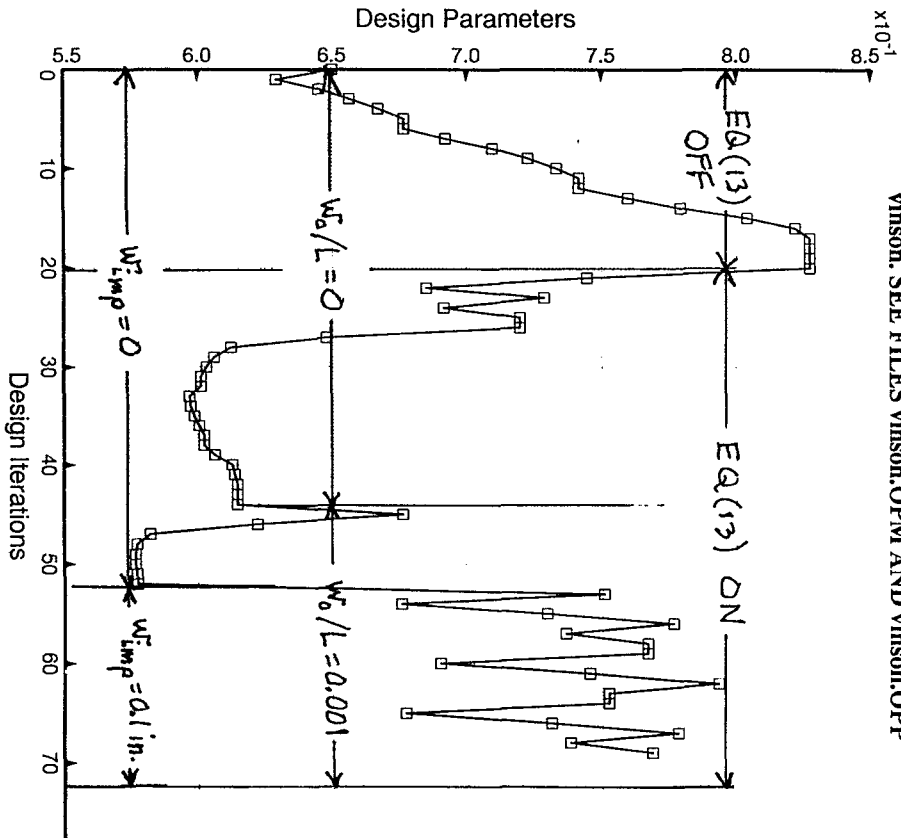vinson. SEE FILES vinson.OPM AND vinson.OPP     vinson. SEE FILES vinson.OPM AND vinson.OPP



Fig. 10 Evolution of honeycomb core thickness
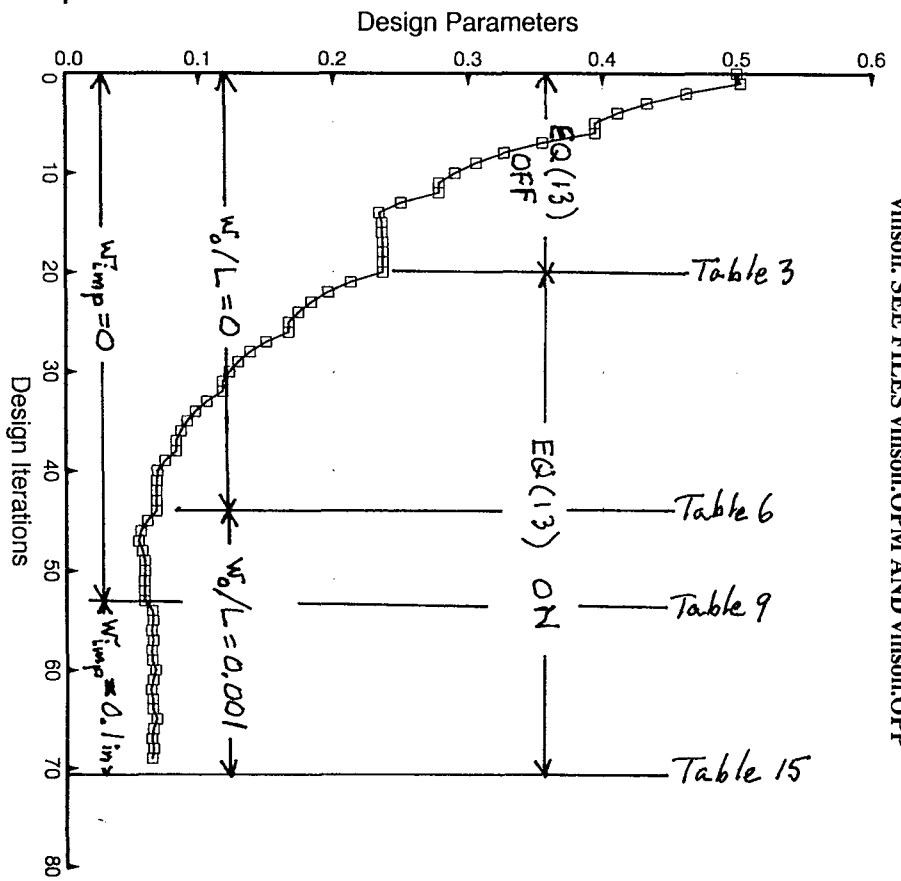


Fig. 11 Evolution of width of one side of
hexagonal honeycomb cell

tc(2 )(SKN):thickness of honeycomb cell wall, tc(2 ): STR seg=1
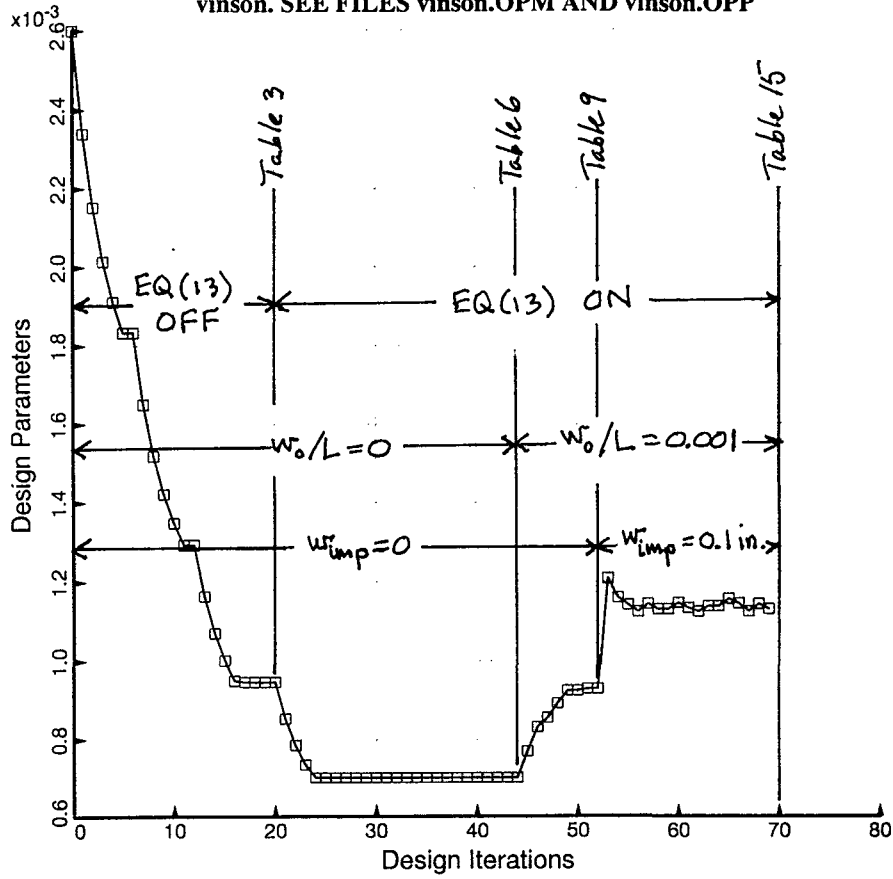
**vinson. SEE FILES vinson.OPM AND vinson.OPP**



Fig. 12 Evolution of thickness of honeycomb
         cell wall